energies

MDPI

Article

Development of a Comprehensive Comparison Software for Automated Decision-Making in Impulse Testing of Power Transformers, Including a Review of Practices from Analog to Digital

Welson Bassi

High Voltage Laboratory, Institute of Energy and Environment (IEE), University of São Paulo (USP), São Paulo 05508-010, Brazil; welson@iee.usp.br

Abstract: Power transformers are fundamental components in electrical grids, requiring robust insulation to operate reliably under various abnormal conditions, including overvoltages caused by lightning or switching. As defined by existing standards, the Basic Insulation Level (BIL) or Switching Insulation Level (SIL) of a transformer validates its reliability through impulse testing. These tests presume linearity in the overall system and equipment being tested. They compare waveforms at reduced and full impulse levels to detect or enhance insulation failures. Traditionally, this relies on visual inspection due to subjective acceptance criteria. This article presents a historical background review of the practices involving the use of analogue instruments evolved into digital oscilloscopes and digitizers, and the ways in which they enhance waveform acquisition and analysis capabilities. Despite advances in digital processing, including analyses on the frequency domain rather than only on time, such as transfer function analysis and coherence functions, and other signal transformations, such as wavelet calculation, interpreting differences in waveform records remains subjective. This article presents the development of a tool designed to emulate traditional photographic methods for waveform comparison. Moreover, the TRIMP software used enables multiple comparisons using various similarity and dissimilarity metrics in both the time and frequency domains, providing a robust system for identifying significant differences. The developed methodology and implemented metrics can form the basis for future machine learning or artificial intelligence (AI) applications. While digital tools offer significant advantages in impulse testing, improve reliability, reduce subjectivity, and provide robust decision-making metrics, their test approval remains based on visual comparisons due to consolidated engineering practices. Regardless of the metrics or indications obtained, the developed tool is a powerful graphic visualizer.

Keywords: power transformer; testing; test; impulse; evaluation; acceptance; significant differences; automated software; machine learning; artificial intelligence; expert system

check for updates

Academic Editor: Isabel Jesus

Received: 17 October 2024
Revised: 13 November 2024
Accepted: 6 December 2024
Published: 2 January 2025

Citation: Bassi, W. Development of a Comprehensive Comparison Software for Automated Decision-Making in Impulse Testing of Power Transformers, Including a Review of Practices from Analog to Digital. *Energies* **2025**, *18*, 156. https://doi.org/10.3390/en18010156

1. Introduction

Power transformers are critical in electrical grids, making their reliability essential across all voltage ratings. The definition of the impulse insulation levels, either the Basic Insulation Level (BIL) or Switching Insulation Level (SIL), is a required parameter in the consolidated methodology adopted over the last century when considering the specification of power transformers and other high-voltage equipment.

These tests deal with lightning and switching overvoltages that transformers might encounter during operation. The higher the insulation levels, the more robust and massive the insulation system is, leading to higher life expectancy and reliability.

This article presents the development of an automated software tool, TRIMP, designed to enhance the evaluation of lightning impulse tests on transformers. The software facilitates the objective comparison of measured signal records, utilizing robust similarity and dissimilarity metrics in both the time and frequency domains. This tool aims to eliminate the subjectivity present in traditional visual evaluations, providing greater precision and reliability in fault diagnostics. Additionally, the software offers the potential to be integrated into future machine learning systems, promoting the continuous evolution in decision-making processes for impulse tests.

Impulse tests became part of technical and commercial agreements in the United States in 1933 [1–3]. However, the AIEE Standard did not initially require impulse tests for dielectric testing [4]. In 1932, about 10% of transformers underwent testing. By 1948, this percentage increased to 60% [5] after the American Standard, ANSI C57.1, C57.2, and C57.3 [6], published in 1942, introduced rules for impulse testing, including examples of impulse tests conducted on the production line as a quality-control tool [7]. The IEC standard addressing this issue first appeared in 1976 [8].

The concept established from the time of the first experiments is to consider that the insulation system and its complex impedance respond linearly to different impulse voltage levels.

In this way, the methodology adopted to verify the intrinsic linearity, and consequently the absence of failure, is to apply impulses on two different levels. One impulse is lower or reduced, and a full one is at the nominal withstand level. Usually, the reduced level is from 50% to 75% of the full-rate impulse test level. Since early times, oscillography records of voltage and currents at both reduced and full levels have been obtained and compared [2,9,10].

Despite almost a hundred years of testing, the evaluation of differences among recorded waveforms is still based on graphical time visualization. The current IEC Standard 60076-3 [11] states that the test successfully passes acceptance "if there are no significant differences between voltage and current transients recorded from the reference impulse and those recorded at the full test voltage".

There are no quantitative or objective criteria to support the interpretation of the test regarding "significant differences" mean. On the standardized procedure of acceptance criteria, the IEC places the note: "The detailed interpretation of the test records and the discrimination between marginal differences and differences indicating failure requires a great deal of skill and experience". Further information given in the specific IEC 60076-4 [12] publication does not help to solve the matter of subjectivity when it states, "This is a skilled task and it is often difficult to decide the significance of discrepancies, even with considerable experience, because of the large number of possible disturbance sources. Discrepancies of any kind are of concern and should be investigated".

With the increased use of digital recorders and enhanced computing capabilities from the 1980s onwards, algorithms and digital processing techniques became possible. Improvements in visual observation assessment emerge when proposing the use of the transfer function technique and of coherence, which works in the frequency domain [12–17].

However, even with the algorithms made possible due to digital processing, the interpretation of changes of $U(\omega)$ and $\mathrm{I}(\omega)$, which are the frequency domain transformations obtained from the time domain signals of voltage $U(t)$ and current $I(t)$, is subjective as stated in IEC 60076-4, once the standard likewise does not establish quantitative admissible numerical differences among records on frequency domain and places the criterion: "Any shift of significant poles in the transfer function is indicative of a part-winding breakdown".

Hence, the golden standard for performing actual impulse tests in a laboratory has remained for over a hundred years: the visual observation of the superposition of the obtained records that tries to identify and explain some significant differences found among them. So, devoted decision-making software or expert systems would automatically deal with this premise [18,19].

Some transformer manufacturers have already utilized the TRIMP software to support decisions on impulse testing. It is a prevalent situation where manufacturers and buyers need some clear, positive, and definite indication regarding the criteria for acceptance of this test. The mere opinion of the test operator based on overall visual evaluation is not always acceptable. Furthermore, this research is likely to be used by the technical committees involved in developing transformer standards, potentially influencing how impulse tests are evaluated.

2. Impulse Test Procedure and Evaluation

This section presents the general methodology, established over previous decades, presenting a historical background of the measurements and equipment deployments.

2.1. General Principle of Impulse Testing

As previously stated, the impulse test premises are based on comparing a set of impulse records in applications of different magnitudes and test conditions. Impulse tests are applied to all high-voltage terminals, with tests on low-voltage and neutral terminals performed according to specific requirements.

Figure 1 illustrates the principle: a reduced intensity full impulse voltage wave (RFW) is applied to produce reference voltage and current traces, as shown in Figure 1a. So, the nominal full impulse voltage (FW) is applied, as shown in Figure 1b. If a failure occurs on the internal winding, as illustrated, there is a corresponding change, for instance, in the current-derived measurement due to changes in the impedance. Figure 1c shows the superposition/normalization of the current traces where one can observe the modification of the current at FW when compared to the reference current RFW.

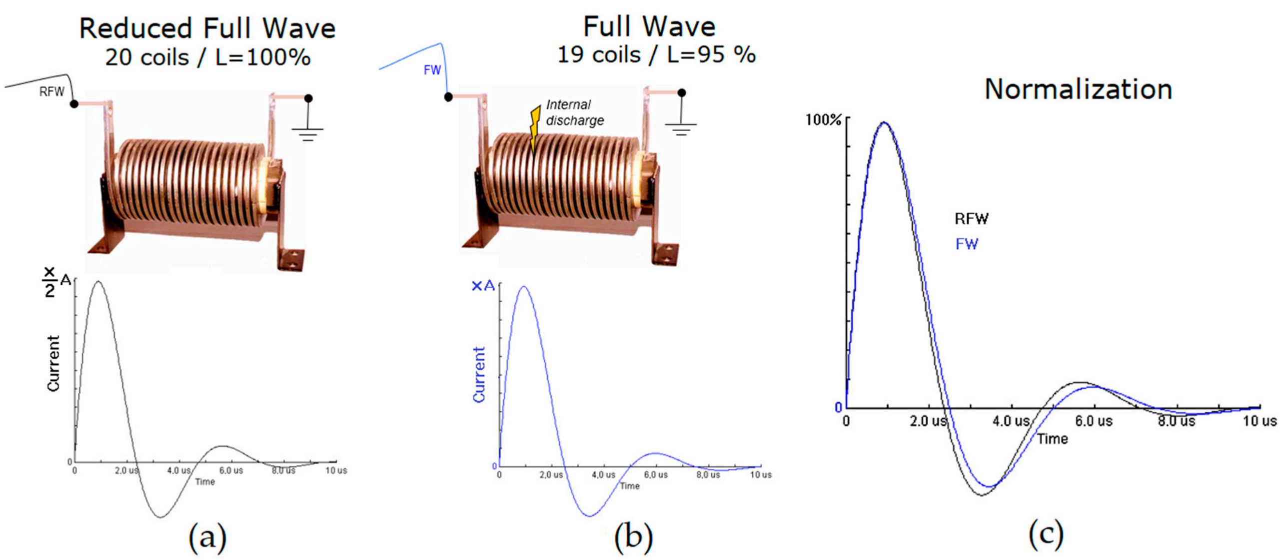

Figure 1. Illustration of general impulse test methodology. (**a**) An impulse application of a reduced full wave (RFW). (**b**) An impulse application of the rated full (FW) wave with an internal failure and (**c**) Normalization to compare both obtained current traces visually.

In addition, the test set considers two types of impulses used: full and chopped. Tailchopped impulses are applied to the standardized tests because of the expected and regular occurrence of sparks and flashovers on the distribution and transmission lines originating fast transients, achieving the transformer terminals. The higher frequency components on the chopped voltages can enhance some previous incipient insulating failures or initiate new ones.

Chopped impulses create high frequencies arising from the abrupt interruption of the high-voltage impulse and can be critical for measurements and comparisons. Since it is tough to keep the same instant of chop on the applied impulses, differences in time to chop are allowed, leading to different responses to the associate voltage and current recorded signals. When the differences in time to chop between two impulses are noticeable, the comparisons are usually performed until the time of the fastest chop.

The standards also require the application of some more full impulses at the rated voltage to verify that any incipient failure has been intensified and become more evident on the records.

The interpretation of the results is based on the assumption that the winding impedance is linear with increasing voltage value and that, except for the scale factor, the records at the two test levels must be identical. Even a tiny local discrepancy indicates a nonlinear behavior of the winding insulation with increasing stress. This nonlinearity is attributed to internal failure.

Along with the tests, other ways to verify the occurrence of failures are used. Visual observation and hearing of arcing, sparking, abnormal noises, and the formation of bubbles in the oil are clear indications of test failure. Voltage collapse or intensity current rising are the most apparent electrical signs of failures on impedance change along the impulse application, more commonly associated with catastrophic or permanent failure.

However, these clear indications do not represent all possible internal failures. Non-permanent or even lasting failures represent a low extension of the insulating system, leading to subtler changes in the oscillography records.

This study deals with lightning impulse tests, but the methodology is quite similar when performing switching tests.

2.2. Historic Background

This section briefly shows how the equipment used for getting the oscillography records and associated standards has evolved over the last hundred years.

The analogue oscilloscope is an electronic instrument used to measure waveforms in electrical circuits. It uses a narrow beam of electrons focused on a fluorescent screen, producing a glowing graph showing the relationship between two or more voltages. Since almost any physical phenomenon can be converted into a corresponding voltage, the oscilloscope is a versatile tool that can be used in all forms of physics research. By 1910, investigations had become sophisticated enough that some means of displaying the surge waveform being produced became a priority. In 1914, Alexandre Dufour was experimenting with placing photographic film in a vacuum chamber and using an electron beam to "write" the image onto the film [20,21]. The vacuum chamber and electron beam eventually became known as a "cathode ray tube" and thus formed the basis of an electronic instrument called an oscilloscope [22]. This project by Dufour was called a "cold-cathode" oscilloscope, and an image of it can be seen in Figure 2a [23,24]. Oscillographs were contemporaneously in increasing use at this time for recording various transients, especially lightning, developed by Norinder [25,26]. The hot cathode oscilloscope eventually replaced the cold cathode oscilloscope. This concept still forms the basis of oscilloscope operation today. A sealed phosphor-coated cathode ray tube is used, and the film used to record the pulse waveform is located in an external camera, as shown in model HC-25 of Figure 2b. Oscilloscopes for high voltage laboratories were developed in the 1950s, e.g., by Tektronix Type 507 in Figure 2c and the Haefely 72 F in Figure 2d.

The digital oscilloscope was developed in 1971 by Hiro Moriyasu (Tektronix), improving upon the old analogue oscilloscope by saving the image in digitized form. LeCroy made the first real-time digital oscilloscope, the model WD 2000, with a memory depth of 20 samples with a breakthrough sampling rate of 1 ns (1 GHz), shown in Figure 2e [26].

By 1980, digital sampling oscilloscopes and digitizers emerged, such as Tektronix programmable digitizers and Nicolet Test Instrument's digital storage oscilloscope.

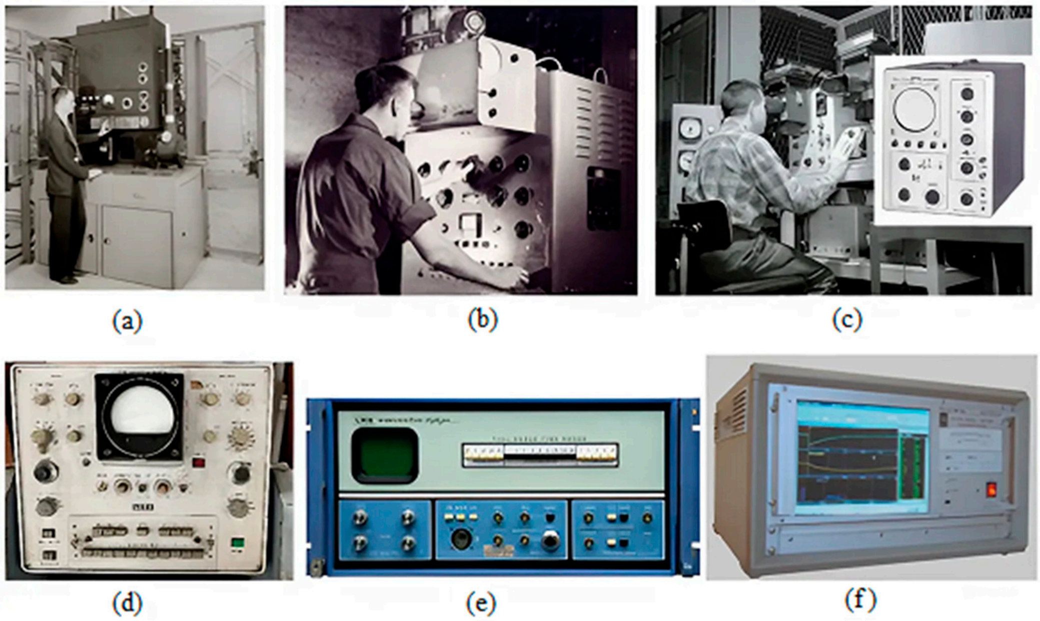

Figure 2. Illustrative overview of the evolution of oscilloscopes and digitizers. (**a**) A Dufour cold-cathode oscillograph type (circa 1920) adapted from [24]. (**b**) Hot-cathode oscilloscope (circa 1940) adapted from [24]. (**c**) Tektronix oscilloscope Type 507 (circa 1950) adapted from [24]. (**d**) Haefely 72 F Oscilloscope (circa 1960) (**e**) Lecroy WD 2000 (circa 1970) [27]. (**f**) Digital Impulse Measuring System used nowadays.

Digital oscilloscopes have become prevalent in most industrial, technical, and scientific applications, but especially in high voltage laboratories when testing transformers; this scenario only occurred in the transition decades of 1990–2000 to nowadays, as displayed in Figure 2f.

Currently, there is a vast commercial offering of digital oscilloscopes with real resolutions of up to 12 bits, PC-oscilloscopes and digitizers with even higher resolutions of up to 14 bits. However, software analysis is still limited when testing power transformers.

In 1987, the Standard IEEE 1122-1987—Standard for Digital Recorders for Measurements in High-Voltage Impulse Tests [28] was issued, recommending a resolution of 0.3% of the peak value when the test requires comparison of records (such as impulse testing). The first edition of the IEC 1083-1 presenting requirements for instruments for impulse tests was issued in 1991 [29] and recommended a rated resolution of 0.2% of the full-scale deviation for tests which require comparison of records. To achieve such requirements regarding the resolution, only oscilloscopes and digitizers of 9 bits or higher of actual resolution or those that are digital should be used. The first software standard, IEC 1083-2, was released in 1996 [30], including, as part of the standard, the software Test Data Generator (TDG) which allows the user to generate digital impulse data with selected resolution and sampling rate [31].

Figure 3a shows an old oscillography photograph obtained from the High Voltage Laboratory of the University of São Paulo, showing two traces corresponding to a reduced full wave (RFW) and a full wave (FW) impulse. Figure 3b shows the total superposition of the two traces, and Figure 3c shows the traces' superposition slightly shifted on the x-axis to demonstrate the existence of the two traces. The process of obtaining the superposition uses an optical multiplier during film development.

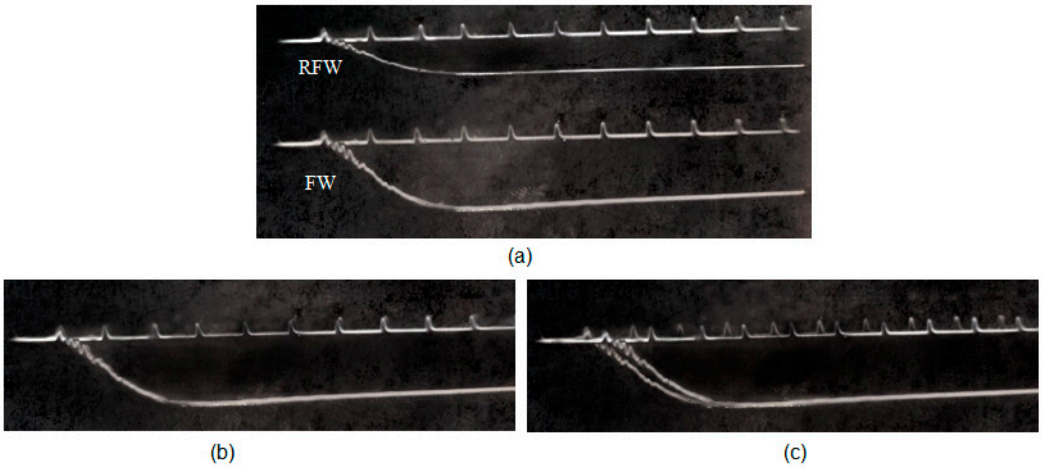

Figure 3. Illustrative view of old photos from HV Lab IEE-USP obtained in an actual impulse test. (**a**) Traces of the RFW and FW. (**b**) Full traces superposition. (**c**) Time-shift on the x-axis of superposed traces.

3. Relevant Aspects of Digital Recording on Impulse Tests

In the context of engineering and signal processing, impulse tests serve as a critical task when analyzing the behavior and characteristics of transformers and reactors. The transition from the oldest analogue instrumentation to current digital records brought a new set of challenges.

Interferences that were not previously detected by analogue oscilloscopes are now captured and recorded and are roughly classified into three categories based on frequency content: test circuit oscillations, electromagnetic interference, and digitizer noise. These three categories have different frequency range characteristics. The test circuit oscillation frequency is often higher than 500 kHz, the electromagnetic interference is usually characterized by frequencies up to several megahertz, and digitizer noise produces frequencies higher than 10 MHz [32].

Higher resolutions, offsets, trigger discrepancies, time shifts, and high-frequency oscillation, for example, can significantly affect the accuracy and reliability of impulse test comparisons [33,34]. Understanding these disturbances and implementing strategies to mitigate their effects is essential for ensuring the integrity of test results.

3.1. Interferences

Discrepancies in timing, synchronization, and electromagnetic interferences represent significant obstacles in impulse testing. Factors such as differences in trigger timing, high-frequency oscillations, and unwanted noise can distort the measured signals, compromising the accuracy of the evaluations.

This section explores some of the primary sources of interference and describes possible effective methods to address these issues, ensuring the reliability of the obtained data:

- Trigger and time-shift discrepancies: manifest as delays or advancements in the recorded signals relative to their expected temporal positions. Accurate timing is critical in impulse testing, determining when the signal is captured and analyzed.

Trigger discrepancies occur when there is a mismatch between the intended trigger point and the actual initiation of data acquisition. This discrepancy can result from signal jitter, latency in trigger circuits, or synchronization issues between multiple measurement devices, mainly due to the impulse generators' and the chopping circuit's stability and control circuits. To mitigate trigger disturbances, precise trigger settings, robust synchronization protocols, and real-time monitoring of trigger events are essential. Commonly, impulse diversity of shapes and intensities produces differences in triggering, resulting in trigger or time-shifted signals, which make comparison and superposition inviable in practice without proper adjustments;

- High-frequency oscillations: often caused by electromagnetic interference or resonances between the generator, the measurement system, and the test object, which can taint impulse test recordings with unwanted noise. These oscillations can obscure signal details, reduce signal-to-noise ratios, and compromise the accuracy of measurements, especially in high-speed digital systems. High frequencies of several megahertz oscillations, much higher than the expected oscillating winding frequency, can be produced by interactions between the transformer under test and the measuring system or by electromagnetic noise due to the sparking on the impulse generator. These oscillations, or noise, can introduce disturbances to the recorded data. Mitigating high-frequency disturbances necessitates effective shielding techniques, noise-filtering mechanisms, and bandwidth adjustments in signal acquisition systems. Differentiating between actual faults and noise requires expertise and some filtering and signal-processing techniques;
- Signal clipping during lightning impulse tests on transformers occurs when transient currents exceed measurement ranges, truncating the waveform and missing the maximum peak and full shape. This clipping occurs due to three overlapping components in the current signal: capacitive, mutual inductance, and main inductive winding components. These components reach their peaks at different times. The capacitive part appears at the waveform's beginning, usually within 10 μs, as capacitances charge and distribute voltage. The mutual inductance component has shorter, slower oscillations up to about 20 μs. The main inductive component exhibits more significant oscillations due to travelling waves in the winding components, peaking after 100 μs in large transformers. Since capacitive peaks occur faster, clipping is common; thus, the maximum clipped capacitive peak should not be used for comparison or normalization. A different scale factor is recommended instead;
- Offset shifts: encountered in electronic systems, refers to a deviation from the expected baseline level of a signal. In impulse tests, the offset can distort the recorded data, leading to inaccuracies in measurements and analyses. The impulse test premise of recording signals at different levels intrinsically leads to using the different gains and scales of the amplifiers, which may be a source of offset due to amplifier imperfections, sensor drift, and electrical interference. Addressing offset disturbances requires careful instrumentation calibration and the implementation of digital corrective algorithms to nullify or compensate the offset values.

3.2. High Resolution

Increased resolution in measurement systems, while offering considerable benefits in detail and data accuracy, also introduces a series of difficulties. These include heightened sensitivity to noise, the need for greater data storage capacity, and the complexity of processing large volumes of information. Additionally, higher sampling rates and susceptibility to calibration and drift require careful management.

Nowadays, very high resolutions are encountered in oscilloscopes (PC-based or standalone) and digitizers. The requirements of the updated standards [29,30] need to be fulfilled. However, new equipment for general applications might need to be carefully planned and proven for high-voltage impulse testing. High-resolution measurements offer the advantage of capturing fine details and mild signal changes, which can enhance the precision and accuracy of detection in various applications. However, a higher resolution can also introduce challenges and complexities that need to be carefully addressed:

- Increased sensitivity to noise: higher resolution means more data points per unit of time or amplitude, making the measurement more susceptible to noise. Even small amounts of noise can become significant relative to the signal in high-resolution measurements, affecting the reliability of detection algorithms and increasing the likelihood of false positives or negatives. Employing robust noise reduction techniques and signal processing algorithms is crucial for maintaining accuracy in the presence of noise;
- Internal noise: the fundamental noise limit is given by the thermal noise voltage generated due to the thermal agitation of electrons described by [35–37]. Plus, internal noise within the measurement system can affect high-resolution accuracy, originating from components like ADCs, amplifiers, or power supplies. This noise impacts low frequencies (below 1 kHz) with flicker noise and high frequencies (over 1 MHz) with quantization noise, especially in high-resolution digitizers. Although generally low in modern devices, internal noise can influence the lower and upper ends of the frequency spectrum. Filtering and signal processing can help mitigate this, ensuring accurate signal capture and analysis;
- Greater data volume: high-resolution measurements result in larger datasets, which can strain computational resources and storage capacities. Processing and analyzing extensive high-resolution data may require advanced computational algorithms and storage optimization. Also, available parallel processing techniques can speed up the processes;
- Higher sampling rates: Higher-resolution measurements typically are followed by higher sampling rates to capture fast-changing or high-frequency signals accurately. However, higher sampling rates can cause signal aliasing and expose the limitations of the sampling hardware;
- Calibration and drift: High-resolution measurement systems are often more sensitive to calibration fluctuations and drift over time. Small changes in instrument calibration or environmental conditions can cause inaccuracies in high-resolution measurements, affecting reliability and repeatability and requiring regular calibration checks, temperature stabilization, and drift compensation techniques.

4. Development of the Implemented Numerical Methodology

As previously mentioned, the assumption of linear behavior of the electrical signals of voltages and currents upon the applied test voltage is the basis of evaluation involved in the methodology of waveform comparisons, as stated in the Standards [11,12].

The digital system must record the test signals and then read, normalize, and have comparison metrics applied by the analysis software. The software development process tested and selected various metrics and numerical methods.

In this section, the numerical methodologies implemented in the software are thoroughly presented and discussed.

The first step in graphical analysis is the accurate acquisition of impulse test records. High-resolution oscilloscopes and/or digitizers are used to capture the waveform characteristics, ensuring that the steep front, peak, and tail are accurately recorded. According to

IEC 60060-1 [38], the sampling rate should be sufficient to capture the transient nature of the impulse waveform [39]. This step precedes the analysis of the signals and, eventually, based on the results obtained in the analyses, adjustments, alterations, or reapplications of the pulses in the test may be necessary.

Once the files are effectively available, they can be opened in the program. By convention, the first file (File 1) is the Reference File (for example, the reduced signs) and the Second file (File 2) becomes the Comparison File. The files are in text format (ASCII) or CSV, as there is no standardized format or protocol for impulse tests on transformers. After reading, the signals are superposed graphically instantly on the x- and y-axis.

The developed software, TRIMP [40], processes the reading of waveform files, and allows the user to normalize them. File 1, or the Reference File (REF), usually consists of values from the reduced waveforms or the initial records of a series of full intensities. File 2, or the Comparing File (COMP), is the one to be compared to. Both waves are scaled by a normalization factor based on two computing methods: direct normalization and normalization by minimizing residues. In the first case, the peak values are found, and normalization is applied between the reference file (REF) and the comparison file (COMP). The response speed in this type of normalization is practically instantaneous. Still, the result may be inaccurate if there are time differences between the peaks of the signals. The second and preferred normalization method adjusts the scale and time shifts of one signal relative to the other, minimizing the residues between them before applying the final normalization. Thus, time and intensities are computed using an optimization algorithm known as Hill Climbing [41]. The algorithm tests incremental adjustments to scale and time shifts to minimize the error between the two signals. The absolute error between the signals is calculated for each combination of adjustments. If a fit results in a smaller error than the previous one, the new value is adopted as the best one found, and the process continues until no better fits are found (indicating that the algorithm has reached a local point of least error).

Automated normalization can ultimately be modified by visually adjusting and moving the waveforms on both axes, and the final visualizing superposition can be achieved for a final decision prior to the numerical parameters' evaluation on the test.

After normalization, the signals are ready to be analyzed in time, and their derived calculations, such as the Fast Fourier Transform (FFT), transfer function, signals coherence, and the wavelet transform, can be derived [12,13,42–45]. Graphical plots fully illustrate all the analyses. Plotting and viewing are critical aspects of making decisions by the experienced people involved in testing.

The final step involves numerical algorithms used by automated tools to compare the test records. In the software developed, statistical indicators and hypothesis tests analyze and quantify the differences between the records, similarly to [46]. Plus, the computer program uses hypothesis tests and critical indicators to provide a more explicit indication of the relevance of such differences. All indicators are based on the comparison metrics with pre-defined default thresholds, shown in this section. However, users can adjust these threshold values and sensitivity.

In summary, the TRIMP software performs manual and automated comparisons of signal records obtained during impulse tests on transformers, providing an objective and comprehensive analysis in both the time and frequency domains. It allows users to normalize signals, shift the waveforms on the x-axis and choose filtering and smoothing algorithms to reduce noise and interference. The software analyzes similarity and dissimilarity metrics in both domains, utilizing Fourier Transform and Wavelet Transform methods. With these functionalities, TRIMP aims to reduce subjectivity in evaluations, offering engineers a robust tool to detect significant differences between tested signals and increasing the reliability of the results.

All numerical algorithms were initially implemented in Python and later converted using MS Visual Studio, allowing the creation of an executable client program to run the application on Microsoft Windows without requiring the interpreter. The software can handle large data files, as presented in the results. There are no specific hardware requirements, but a faster processor and as much system memory as possible will enhance the software's performance.

4.1. Metrics for Evaluation of Similarity (Or Dissimilarity)

Data analysis and signal comparison are crucial in various research and engineering fields, including impulse testing in transformers. Researchers use multiple metrics or distances to quantify the differences or similarities between datasets or signals. The book [47] lists and presents more than 1400 named distance expressions for different applications, emphasizing infinite possibilities. Selecting, implementing, and verifying the applicability of mathematical expressions and algorithms is a monumental task.

One can classify these metrics into three main categories: dissimilarity, similarity, and statistical measures. Additionally, these metrics apply to both the time and frequency domains in the context of electrical signals. Each category has unique characteristics and applications, providing specific insights and results for the data analyzed.

The selection and testing of metrics are fundamental stages during the research. Below are synthetic presentations and corresponding expressions of those metrics selected and used in the developed computational program.

4.1.1. Statistical Measure

Statistical tests are widely used for evaluating differences between signals, helping to determine if observed variations are significant or merely due to random chance. The tests reveal critical values capable of rejecting the null hypothesis, which states that there is no difference between the signals under evaluation. Among these tests are the *t*-test and *z*-test.

The *t*-test compares the means of two small populations to determine if they significantly differ, especially when sample sizes are around a few dozen, and the population standard deviation is unknown. In contrast, the *z*-test suits larger populations with known standard deviations. A significance level of $\alpha = 0.05$ (95% confidence) sets the null hypothesis ($H0$) that the means are statistically equal, signifying no significant difference. If the calculated t- or z-statistic exceeds the critical value, one rejects $H0$, indicating a significant difference. For the *z*-test, the critical value for 1000 degrees of freedom or more is approximately 1.96. In this study, the *t*-test applies to frequency domain analysis with around a hundred samples, using a critical value of about 1.984 to reject $H0$.

The expressions for the tests:

$$z = \frac{\overline{x} - \overline{y}}{\sqrt{\frac{n_x\sigma_x^2}{n_x} + \frac{n_y\sigma_y^2}{n_y}}} \text{and } t = \frac{\overline{x} - \overline{y}}{\sqrt{\frac{s_x^2}{n_x} + \frac{s_y^2}{n_y}}} \tag{1}$$

where: $\overline{x}$ and $\overline{y}$ are the means, σ_x^2 and σ_y^2 are the variances, and n_x and n_y are the sample sizes of $x(t)$ and $y(t)$, respectively.

4.1.2. Similarity Measures

Similarity metrics are mathematical tools used to quantify the degree of resemblance between two or more signals, such as voltage or current waveforms. In the context of impulse transformer testing, these metrics are essential for automating the evaluation of the test results. By comparing signals, similarity metrics help identify minor deviations that might indicate potential issues while confirming when no significant differences exist.

The selected and implemented metrics for similarity measures are:

- Coefficient of Determination;
- Concordance Correlation Coefficient;
- Cosine Similarity.

The Coefficient of Determination (R^2) measures the proportion of variance in the data that is explained by the correspondence between two signals. A value of 1 indicates that the relationship between the signals explains all variance, and 0 indicates that there is no correspondence between the signals $x(t)$ and $y(t)$. The expression for R^2 is:

$$R^2 = 1 - \frac{\sum_{i=1}^{n}(x_i - y_i)^2}{\sum_{i=1}^{n}(x_i - \overline{x})^2} \tag{2}$$

The developed TRIMP software uses a threshold value for R^2 of 0.9 (default). Values below this limit indicate that the signals differ significantly.

The Concordance Correlation Coefficient (CCC) measures the agreement between two data sets, quantifying how closely the observed data align with the line of perfect concordance $x = y$ when comparing signals $x(t)$ and $y(t)$. It extends the concept of correlation by incorporating both the Pearson correlation coefficient and mean–variance equality. The Pearson Correlation Coefficient (ρ) indicates the strength of the linear relationship between two variables, ranging from -1 to 1, where 1 signifies a perfect positive linear relationship, 0 indicates no linear relationship, and -1 represents a perfect negative linear relationship.

In the case of, $x(t)$ and $y(t)$, ρ is defined as the CCC expression is:

$$\mathrm{CCC} = \frac{2\rho\sigma_x\sigma_y}{\sigma_x^2 + \sigma_y^2 + \left(\mu_x - \mu_y\right)^2}, \text{ being } \rho = \frac{\mathrm{Cov}(x,y)}{\sigma_x\sigma_y}$$

where $\mathrm{Cov}(x,y)$ is the covariance between $x(t)$ and $y(t)$, σ_x and σ_y are the standard deviations and μ_x and μ_y are the means of $x(t)$ and $y(t)$, respectively.

Transforming the Concordance Correlation Coefficient (CCC) to a range of 0 to 1 offers advantages by creating a more intuitive scale of similarity or agreement. This adjustment aligns with other metrics, provides a clearer representation of discordance, and simplifies thresholding and decision making, reducing the risk of misinterpretation. A specific transformation can be applied to ensure that the CCC always falls within the range [0, 1], where 1 indicates perfect concordance, and 0 indicates perfect discordance.

$$\mathrm{CCC} = \frac{1 + \frac{2\rho\sigma_x\sigma_y}{\sigma_x^2 + \sigma_y^2 + \left(\mu_x - \mu_y\right)^2}}{2} \tag{3}$$

In the developed TRIMP software, values of CCC below 0.9 (default) indicate that the signals present significant differences.

Cosine similarity is a measure between two non-zero vectors in a multi-dimensional space. It is calculated by taking the cosine of the angle between the two vectors. The cosine of 0° is 1, meaning that if the vectors point in the same direction, the cosine similarity is 1, indicating perfect similarity. If the vectors are orthogonal (i.e., the angle between them is 90°), the cosine similarity is 0, indicating no similarity.

When two sampled signals are $x(t)$ and $y(t)$, the cosine similarity is given by:

$$\text{Cosine Similarity} = \frac{\sum_{i=1}^{N} x_i \cdot y_i}{\sqrt{\sum_{i=1}^{N} x_i^2} \cdot \sqrt{\sum_{i=1}^{N} y_i^2}} \tag{4}$$

where N is the number of samples.

A cosine similarity value below 0.9 (default) indicates significant differences between the signals in the TRIMP software.

4.1.3. Dissimilarity Measures

Dissimilarity measures are analytical techniques designed to assess the degree of variation between distinct objects, such as variables, vectors, signals, or data points. Unlike similarity metrics, which focus on commonalities, dissimilarity measures emphasize the distinctions and variations that set entities apart. By focusing on the differences, dissimilarity measures can uncover refined irregularities that might signal underlying issues. This targeted analysis is essential for determining whether significant differences exist among the compared signals.

The selected and implemented metrics for dissimilarity measures are:

- Average Difference;
- Mean Absolute Error;
- Root Mean Square Error;
- Normalized Euclidean Distance;
- Total Harmonic Distortion (THD) Difference (applied in the FFT Analysis);
- Dynamic Time Warping (applied in the Time Analysis).

The Average Difference when comparing two signals is simple to calculate and provides a basic sense of central tendency, making it a convenient tool for initial comparisons. It gives a quick snapshot of overall levels and is a foundational component for other calculations. However, the simple average has limitations; it does not account for variations within the signals and can be misleading if there are significant deviations or noise. Outliers can heavily influence the average, potentially distorting the representation of the central tendency.

Establishing a threshold to determine signal differences is challenging, as it requires considering signal variability, context, and appropriate statistical methods. Based on experimentation considering natural variations of signals and overlapping noises, a threshold of a 10% (default) difference between the arithmetic average between measured values has been chosen in the developed software as an indication of significant differences between the signals. Nevertheless, combining the other implemented metrics makes the overall evaluation process more robust.

The corresponding expression of Average Difference (AD) between two signals $x(i)$ and $y(i)$ in percentage terms is:

$$\mathrm{AD} = \frac{1}{N}\sum_{i=1}^{N}\left|\frac{x_i - y_i}{x_i}\right| \times 100 \tag{5}$$

where N is the number of sampled points.

Mean Absolute Error (MAE) calculates the mean of the absolute differences between each pair of corresponding values of two signals. This metric is conceptually simple and straightforward; it is simply the average absolute vertical or horizontal distance between each point in a scatter plot and the $Y = X$. Even if the signals are pretty similar, MAE can highlight slight but consistent differences that might be important, as well as their relative insensitivity to outliers compared to average or other error-squared metrics. It can be expressed as:

$$\mathrm{MAE} = \frac{1}{N}\sum_{i=1}^{N}|x_i - y_i| \tag{6}$$

where N is the number of sampled points.

A MAE value higher than 10% (default) is considered an indication of a significant difference between the records in the software.

Root Mean Square Error (RMSE) is another widely used metric which is particularly useful when one wants to emphasize more significant errors, as it calculates the square root of the mean of the squares of the differences between signals $x(i)$ and $y(i)$. Due to its sensitivity to significant errors, RMSE can be significantly inflated due to outliers. This makes this metric more conservative than the previous ones, more informative about the worst-case scenario, and more appropriate for emphasizing the larger differences. Its expression:

$$\mathrm{RMSE} = \sqrt{\frac{1}{N}\sum_{i=1}^{N}(x_i - y_i)^2} \tag{7}$$

where N is the number of sampled points.

A value of 0 for RMSE indicates a perfect fit and higher values indicate greater deviations relative to the mean of the data. In the software, a value higher than a threshold of 10% (default) flags the indication of significant differences.

Euclidean distance, a fundamental concept in geometry, measures the straight-line distance between two points based on the Pythagorean theorem, which states that in a right-angled triangle, the square of the hypotenuse is equal to the sum of the squares of the other two sides. This concept generalizes to higher dimensions, forming the basis for a family of metrics known as L_2 norms or Euclidean norms. The Normalized Euclidean Distance (NED) measures the Euclidean distance between two signals, normalized by a factor. Considering the distance in multidimensional space, this metric offers a geometric measure of dissimilarity when it is necessary to consider the dimension of the signals for a fair comparison. The mathematical expression between two signals $x(i)$ and $y(i)$ is:

$$\mathrm{NED} = \frac{\sqrt{\sum_{i=1}^{N}(x_i - y_i)^2}}{\sqrt{\sum_{i=1}^{N}\left(x_i^2 + y_i^2\right)}} \tag{8}$$

where N is the number of sampled points.

The Normalized Euclidean Distance (NED) ranges from 0 to 1, where zero indicates that the two vectors are identical and there is no difference. In contrast, one indicates that the vectors are as different as possible according to the normalization.

A NED value higher than the value of 0.1 (default) is an indication of significant differences in the developed software.

Total Harmonic Distortion (THD) indicates the difference in total harmonic distortion between two signals on the frequency domain related to distortion in a signal due to harmonics. It is typically expressed as a percentage and can be calculated using the Fourier components of a signal. In the context of signals $x(\omega)$ and $y(\omega)$ in the frequency domain, the individual THD and the THD Difference in percent can be calculated from the Fast Fourier Transform (FFT) components, expressed as:

$$\begin{gathered}\mathrm{THD1} = \frac{\sqrt{\sum_{\omega=2}^{N}(x(\omega))^2}}{x(1)},\ \mathrm{THD2} = \frac{\sqrt{\sum_{\omega=2}^{N}(y(\omega))^2}}{y(1)} \\ \mathrm{THDDiff} = \left(\frac{\mathrm{THD1}-\mathrm{THD2}}{\mathrm{THD1}}\right) \times 100\end{gathered} \tag{9}$$

The critical default level of THD Difference of 10% (default) is set to consider the FFT components significantly different between the records.

Dynamic Time Warping (DTW) is a powerful technique used to measure the similarity between two time-dependent sequences, that may vary in speed or timing. It was originally created for speech recognition [48]. DTW is particularly useful when sequences are similar but not perfectly aligned, as it accounts for shifts and timing differences between them [49,50]. DTW "warps" the time axis of one sequence to match the other, allowing a more accurate comparison than Euclidean distance. It computes the cumulative distance after optimally aligning two sequences in time. A smaller DTW value means the sequences are more similar, while a larger value indicates more significant dissimilarity, quantifying how much one sequence needs to be warped to match the other

Mathematically, DTW calculates the optimal alignment between two sequences by minimizing the cumulative distance between corresponding points after warping. Given two sequences, $X = [x1, x2, \ldots, xn]$ and $Y = [y1, y2, \ldots, ym]$, DTW seeks to find a warping path that aligns these sequences in a way that minimizes the overall distance. The cumulative distance $D(i,j)$ at each point along the path is computed recursively using the equation:

$$D(i,j) = \mathrm{dist}(x_i, y_j) + \min\{D(i-1,j), D(i,j-1), D(i-1,j-1)\} \quad (10)$$

where $\mathrm{dist}(x_i, y_j)$ is the distance between the points x_i and y_j.

The basic algorithms for calculating DTW are founded on the computation of the distance Matrix between the two-time series. Its computational complexity can be high, making long sequences very slow and computationally intensive. One common technique to speed up DTW is a windowing approach. The Sakoe–Chiba band is the windowing technique employed in the software [51].

In order to illustrate how DTW is highly sensitive to changes in time signals, a practical experiment is presented. Oscillatory damped voltages were measured, as shown in Figure 4a. Signal-1 has a 100 V peak with a natural frequency of 100 kHz, while Signal-2 is 10% less intense, resulting in a 90 V peak. It is clear the signals have significant differences. Analytical calculations suggest a maximum average difference of 10% between the signals; however, random noise affects these expectations. Several metrics, including DTW, were used to evaluate the numerical dissimilarities between the signals. The DTW Paths illustrate how points in one signal correspond to points in another, even if not time-aligned. The red dashed lines show these dynamic alignments, enabling flexible matching despite temporal differences.

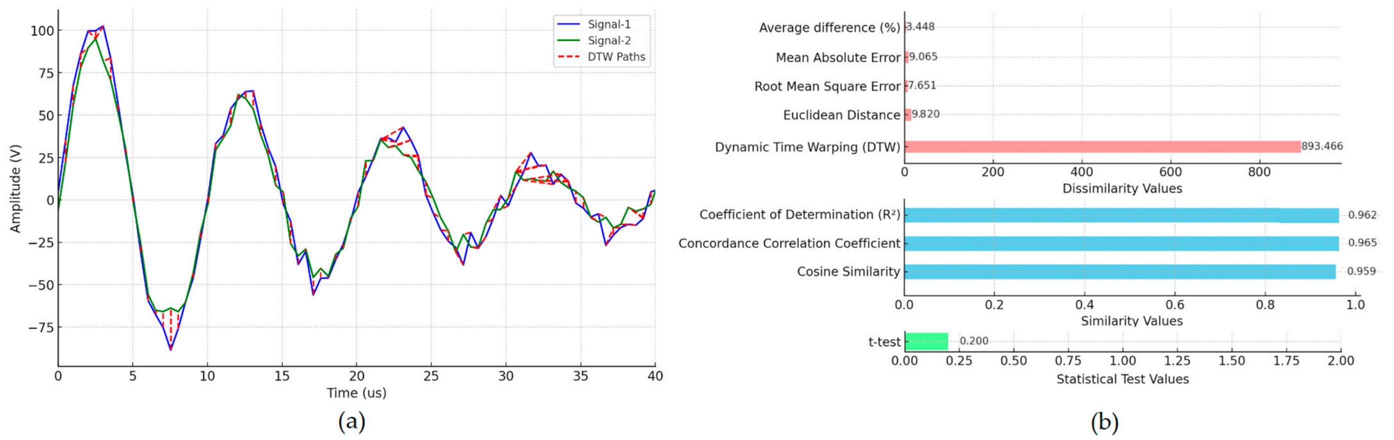

Figure 4. (**a**) Illustration of the calculated DTW (Dynamic Time Warping) paths between two signals. (**b**) Comparison of various metrics of similarity and dissimilarity between the two signals.

Figure 4b displays the calculated metrics for the signals. The high sensitivity of the DTW distance is evident. However, the other metrics and the *t*-test indicate substantial signal agreement.

In the TRIMP software, the approach is to normalize DTW, dividing the DTW distance by the series length to get a per-point distance. If the Normalized DTW Distance is higher than the threshold value of 1.1 (default), the signals are considered to have significant differences.

4.2. Numerical Evaluation in Time Domain

The recommended initial approach for analyzing similarity between test signals is time-domain analysis. These analyses are performed directly on the input signal vectors, the impulse test's current or voltage signal records in transformers, normalized, but without any transformation in the frequency domain.

The applied metrics on the time domain module are those presented in the numerical expressions (1)–(8) and (10).

The metrics are presented at the end of the processing, and the percentage differences are plotted. Based on the results, a message indicates significant or no differences between the signals in time.

4.3. Numerical Evaluation in Frequency Domain

Frequency domain analysis is a powerful technique widely used in understanding and interpreting signals, particularly in telecommunications, audio processing, and electrical engineering. By transforming a signal from the time domain to the frequency domain, one can gain insights often not visible when analyzing the signal in its original form.

In the frequency domain, the signal is represented by its constituent frequencies, allowing for the identification of key characteristics such as dominant frequencies, bandwidth, and harmonic content. This is particularly useful in applications where the behavior of a system or signal is more easily understood in terms of frequency rather than time.

Fast Fourier and Wavelet transform techniques are used to decompose the waveform into frequency components, providing a detailed graphical representation.

4.3.1. Fast Fourier Transform (FFT)

Frequency domain analysis is determined by transforming a signal from the time domain into the frequency domain using mathematical transformations, the most common of which is the Fourier Transform. The Fourier Transform decomposes a time-domain signal into its constituent sinusoidal components, each with a specific frequency, amplitude, and phase. This is often done for discrete signals using the Discrete Fourier Transform (DFT), which is efficiently computed via the Fast Fourier Transform (FFT) algorithm. The transformation results originate a frequency spectrum visualization that displays the signal's amplitude across different frequencies, providing insight into the signal's frequency content.

The Fast Fourier Transform (FFT) is a fundamental tool in signal analysis, mainly when dealing with impulses that have high-frequency components converting a signal from the time domain to the frequency domain, allowing the frequency components of the signal to be analyzed in detail. The FFT is an efficient implementation of the Discrete Fourier Transform (DFT), which calculates the frequency components of a signal. For a signal $x(t)$ with N samples, the DFT is defined as:

$$X(k) = \sum_{n=0}^{N-1} x(k) \cdot e^{-j\frac{2\pi}{N}kn} \tag{11}$$

where $X(k)$ represents the frequency components in the frequency domain. $x(k)$ is the signal value in the time domain; k is the frequency index and N is the total number of samples.

The algorithm implemented in the developed TRIMP software is the Cooley–Tukey [52], which splits a DFT of size N into two smaller DFTs of size $N/2$ at each step. The algorithm reduces the computational complexity of the DFT, making the process more efficient, especially for long signals, and the resulting outputs are complex-valued frequency-domain representations of these signals.

Once the FFT is available, the metrics are applied and calculated according to the numerical expressions (1) to (9) and properly presented.

4.3.2. Coherence Function

Still, in the frequency domain, from the calculated FFT components, the coherence function between the vectors can be computed for the signals from the transformer [53].

The coherence function $C_{xy}(f)$ between the two signals $x(t)$ and $y(t)$ is defined as:

$$C_{xy}(f) = \frac{S_{xx}(f) \cdot S_{yy}(f)}{\left|S_{xy}(f)\right|^2} \tag{12}$$

where $S_{xy}(f)$ is the cross-spectral density between $x(t)$ and $y(t)$, $S_{xx}(f)$ is the power spectral density of $x(t)$, $S_{yy}(f)$ is the power spectral density of $y(t)$ and, $\left|S_{xy}(f)\right|^2$ represents the magnitude squared of the cross-spectral density.

Coherence measures the extent to which signals share common frequency components, considering amplitude and phase differences. It is a valuable tool for analyzing the relationship between signals in the frequency domain, helping to identify shared characteristics and dependencies across frequency ranges. The function ranges from 0 to 1. A value near 1 indicates a strong linear relationship at a specific frequency, while a value near 0 suggests no linear correlation.

In the developed TRIMP software, the coherence function is plotted alongside the FFT visualization of the signals. If the average coherence is below 0.9, the signals are considered to have significant differences.

4.3.3. Transfer Function

A transfer function describes the linear relationship between the input and output of a system or component, such as the transformer [54]. Short and pictorial presentations of the technique are placed in the current edition of the Standard IEC [11,12]. The standard states that the time records of both the applied voltage $U(t)$ and the corresponding impulse current $I(t)$ can be transformed using the Fast Fourier Transformation (FFT) to the frequency domain being, respectively, $U(\omega)$ and $I(\omega)$ and their spectra can be processed to derive the impedance or admittance functions.

Once the Discrete Fourier Transform (DFT) calculates the frequency components of the applied voltage and current, $U(k)$ and $I(k)$, the impedance transfer function is implemented in the developed software by using the relation:

$$Z[k] = \frac{U[k]}{I[k]} \tag{13}$$

where, $Z(k)$, $U(k)$ and $I(k)$ represents the corresponding quantities on the k frequency components in the frequency domain.

The magnitudes of the components of $Z(k)$ are compared using metrics based on the numerical expressions (1) to (8).

4.3.4. Wavelet Transform

Wavelets are mathematical functions that analyze signals by breaking them into manageable parts to identify frequency components at various scales. Unlike Fourier transforms, which use sine and cosine functions, wavelets employ localized wave-like functions that vary in scale and position [55,56]. This allows for simultaneous time and frequency analysis, detecting changes across time or frequency bands. Introduced by Morlet in the 1980s [57], wavelets decompose signals into frequency components tied to specific scales. The TRIMP software uses the discrete wavelet transform (DWT) [58,59], which decomposes signals into high-frequency details and low-frequency approximations using the Haar wavelet [60,61]. Based on the chosen wavelet, low-pass and high-pass filters extract these components.

Mathematically, the decomposition of the discrete-time signal $x(k)$ is performed in a combination of approximation coefficients A and scaling functions ϕ, as well as a sum of detail coefficients D and wavelet functions ψ according to the following expression:

$$x[k] = \sum_m A_{j_0}(m)\phi_{j_0,m}[k] + \sum_{j=j_0}^{\infty}\sum_m D_j(m)\psi_{j,m}[k] \tag{14}$$

where:

$x[k]$ represent the discrete-time signal,
$\phi_{j_0,m}[k]$ is the scaling function at scale j_0 and position m, evaluated at time index k,
$\psi_{j,m}[k]$ is the wavelet function at scale j and position m, evaluated at time index k,
$A_{j_0}(m)$ are the approximation coefficients at scale j_0 and,
$D_j(m)$ are the detail coefficients at scale j.

The approximation $A1$ is obtained by convolving the signal with the low-pass filter and then downsampling (i.e., reducing the sampling rate by half). The details $D1$ are obtained by convolving the signal with the high-pass filter and similarly downsampling. This process can be repeated by further decomposing each approximation into new approximations and details (e.g., $A2$, $D2$), creating a series of increasingly detailed levels of resolution.

In the developed TRIMP software, the methodology has established three frequency bands, leading to six levels of wavelet decompositions, with the corresponding frequency ranges shown in Table 1. Analogous to the FFT, the maximum frequency that can be accurately represented in wavelet decomposition is still limited to half of the sampling frequency, per Nyquist's theorem. Therefore, the limits in Table 1 represent the maximum values contingent upon the sampling frequency of the recorded signals.

Table 1. Frequency ranges on selected bands in wavelet analysis.

Frequency Bands	Approximation Coefficients	Detail Coefficients
High Frequency Band (HF)	500 kHz	1 MHz
Medium Frequency Band (HF)	250 kHz	500 kHz
Low Frequency Band (LF)	50 kHz	100 kHz

The coefficients A (representing approximation coefficients) and D (representing detail coefficients) result in vectors used to compare signals through metrics employed in both FFT and time domain similarity and dissimilarity calculations. A and D are compared using the metrics outlined in numerical expressions (1) to (8). The worst cases, which show the greatest asymmetries or lowest correlations, are then assessed against predefined critical levels to determine whether the signals exhibit significant differences.

4.4. Digital Signal Pre-Processing

When conducting digital measurements on high voltage impulse tests on transformers, noise can significantly impact the accuracy and reliability of the data obtained. The electrical environment during these tests is inherently noisy, influenced by factors such as electromagnetic interference (EMI) and switching, and sparks on the high-voltage impulse generator. Concurrently, signal recordings with an inappropriate signal/noise ratio occur, for instance, when the magnitude of the measured signal is significantly lower than the full scale selected on the digitizer or oscilloscope. In addition to interference, different offset values may occur due to characteristics involved in digitization.

In order to observe the baselines and overall comportment of the signals in the lower frequencies presumed for the winding's responses, digital low-pass signal processing and offset difference removal algorithms are implemented in the TRIMP software. Therefore, the user can choose to apply these algorithms to improve the presentation signals for comparisons.

4.4.1. Offset

Since reduced and full pulses invariably appear at different scales and gains on the digitizer or oscilloscope, different offset values may be recorded for the signals. When offset errors are present in the sampled signals, comparisons will show these differences, leading to misleading indications of significant differences between the records. Generally, these offset errors become apparent only when comparing files, exactly as in impulse tests on transformers.

The TRIMP software allows equalizing the offsets between the files by aligning the average values of the initial flat portions of the records.

4.4.2. Smoothing

A smoothing algorithm effectively reduces the impact of noise in the signal. The algorithm can attenuate high-frequency noise components that obscure the underlying signal by averaging or weighting nearby data points.

The signal smoothing is performed on the developed TRIMP software using a weighted moving average algorithm. The equation for the weighted moving average to calculate the smoothed value of the point $p(n)$ based on its five precedent and five subsequent values, with weights represented as $W_{-5}, W_{-5}, \ldots, W_{-1}, W_0, W_1, \ldots, W_5$, can be formulated as:

$$p(n) = \frac{\sum_{k=-5}^{5} W_k \cdot p(n+k)}{\sum_{k=-5}^{5} W_k} \tag{15}$$

where, $p(n)$ is the value of interest at index n, $p(n+k)$ represents the values of the series at indices $n-5$ to $n+5$ and, W_k are the weights assigned to each of these values; the assigned weights W_k, from $k = -5..5$ are 1, 1, 2, 3, 4, 5, 4, 3, 2, 1, 1, respectively.

4.4.3. Digital Filtering

As mentioned in Section 3, high-frequency unsought oscillations and noise can frequently be imprinted on the measurements. So, in the developed TRIMP software, a digital filter algorithm is implemented so the user can select and apply a cutoff frequency to the signals.

The filter is based on Chebyshev [62,63] polynomial coefficients filtering, and the algorithm involves some steps including: establishing the cutoff frequency and a pre-warping factor, calculation of the normalization factor and the filter coefficients before applying the filtering operation.

5. Results

Testing the methodology for automating impulse test comparisons is essential to ensure accuracy, reliability, and applicability across various transformer types. With a vast array of transformers, from small devices to large power transformers with diverse power ratings and voltage levels, selecting appropriate test cases poses a significant challenge.

Hundreds of records were tested during development to ensure the automated system's robustness in decision making, accounting for the wide variety of transformer types and operational conditions it may encounter.

This section presents selected test cases to illustrate the methodology's application and demonstrate its effectiveness with different transformers. These cases encompass a broad spectrum of power ratings, voltage levels, and operational conditions, showcasing how the system accurately processes diverse scenarios in actual impulse tests.

Each test case begins with a brief description of the test object, followed by the actual results—specifically, whether the records indicate significant differences based on visual comparisons. Test cases include voltage and current waveforms with full and chopped impulses.

During the results presentation, the following nomenclature is used referring to the modules presented in the automated TRIMP software: TIME (Time Domain Analysis), FFT (Frequency Domain Analysis and Coherence Function), TF (Transfer Impedance Function Analysis), and WT (Wavelet Transform Analysis).

Table 2 summarizes the results.

Table 2. Summary of the results.

Test Case	Transformer Data	Sampling Rate/ Resolution/ Number of Samples	Visual Inspection Result	TRIMP Modules Results
1	30 MVA, 145 kV/13.8 kV, BIL 550 kV, Terminal H1	250 MSamples/s 10 bits 20 kSamples	No significant differences in voltage and current records.	No significant differences across all modules: TIME, FFT, TF, WT.
2	30 MVA, 145 kV/13.8 kV, BIL 550 kV, Terminal H3	250 MSamples/s 10 bits 20 kSamples	Significant differences in voltage and current records.	Voltage: Significant differences in TIME and WT; Current: Significant differences in all modules: TIME, FFT, TF, WT.
3	10 MVA, 69 kV/13.8 kV, BIL 325 kV/110 kV, Terminal X1	250 MSamples/s 10 bits 15 kSamples	Significant differences in current comparison	Voltage: No significant differences; Current: Significant differences in FFT, TF, WT.
4	1000 kVA,13.8 kV/0.6 kV, BIL 110 kV, Terminal H1 Dry Type	75 MSamples/s 9 bits 32 kSamples	No significant differences, but notable offset displacement.	Before offset adjustment: Significant differences in TIME and WT; After offset adjustment: No significant differences across all modules.
5	45 kVA, 13.8 kV/0.22 kV, BIL 110 kV, Terminal H2	120 MSamples/s 12 bits 2.4 kSamples	No significant differences in chopped impulse comparison.	No significant differences across all modules: TIME, FFT, TF, WT.
6	500 kVA, 13.8 kV/0.22 kV, BIL 110 kV, Terminal H1	250 MSamples/s 10 bits 20 kSamples	Significant differences observed after chopping.	Significant differences in all modules: TIME, FFT, TF, WT.
7	500 kVA, 13.8 kV/0.22 kV, BIL 110 kV, Terminal H1	250 MSamples/s 10 bits 20 kSamples	No significant differences before the fastest chop event.	No significant differences across all modules: TIME, FFT, WT.
8	1000 kVA, 15 kV/0.22 kV, BIL 125 kV, Terminal X1	250 MSamples/s 10 bits 32 kSamples	No significant differences, but noise hinders visualization.	TIME and WT indicate significant differences before filtering. After filtering, no significant differences across all modules.

5.1. Test Case 1—Transformer 30 MVA—Terminal H1

Test case 1 refers to an impulse test on a three-phase transformer 30 MVA, Dy, 145 kV/13.8 kV, BIL 550 kV/110 kV, terminal under test H1. Voltage and current were sampled at 250 MSamples/s, 10 bits-resolution, 20 kSamples.

Visual inspection confirms no significant differences across all voltage and current records. The TRIMP software indicates no significant differences in all modules: TIME, FFT, TF, and WT.

Figure 5 shows all the module's screen captures.

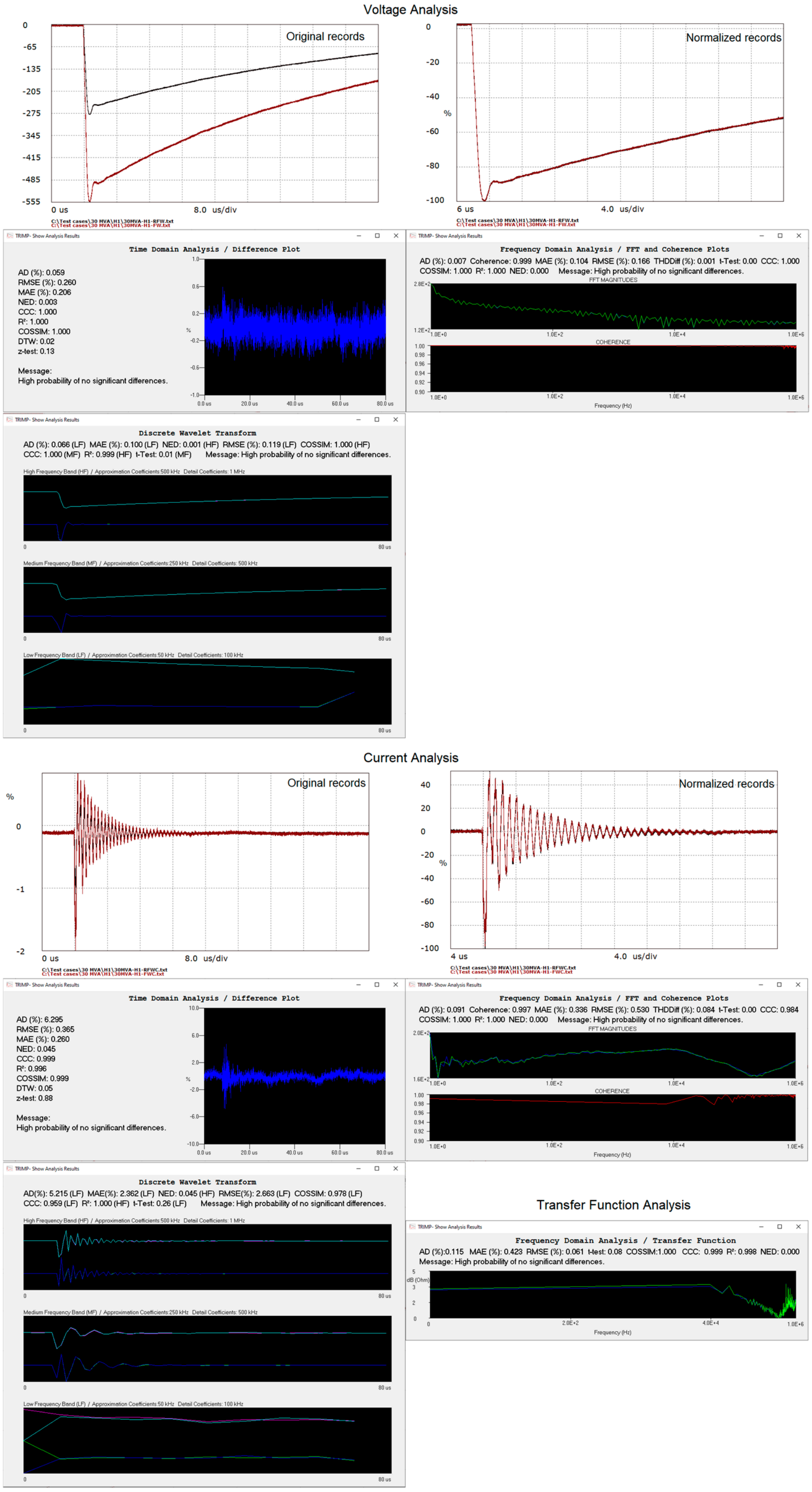

Figure 5. TRIMP software screen captures for Test Case 1. Different colored lines represent calculations for reduced and full impulses.

5.2. *Test Case 2—Transformer 30 MVA—Terminal H3*

Test case 2 refers to the same Test Case 1 transformer but testing the terminal H3. Visual inspection confirms significant differences in the voltage and current records.

Normalization reveals a slight but noticeable difference in the voltage comparison at the peak region. For the voltage signal comparison, the TRIMP software indicated a significant difference only in the TIME module due to the DTW metric, and in the module WT. The automated TRIMP software indicates significant differences in all modules: TIME, FFT, TF, and WT for the current signals.

Figure 6 shows all the module's screen captures.

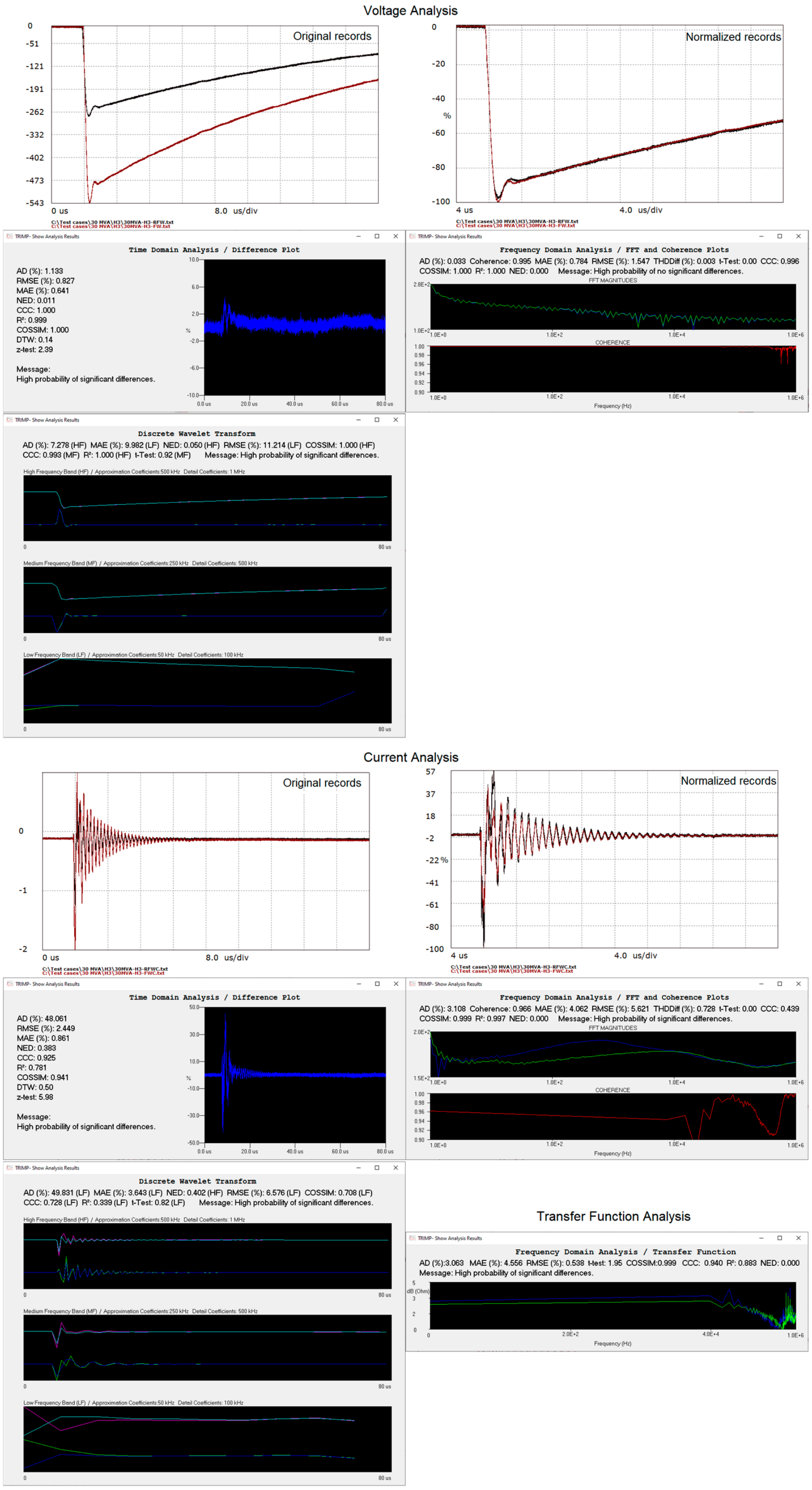

Figure 6. TRIMP software screen captures for Test Case 2. Different colored lines represent calculations for reduced and full impulses.

5.3. Test Case 3—Transformer 10 MVA—Terminal X1

Test case 3 refers to an impulse test on a three-phase transformer 10 MVA, Dy, 69 kV/13.8 kV, BIL 325 kV/125 kV. The terminal under test is the low-voltage side terminal X1. Voltage and current were sampled at 250 MSamples/s, 10 bits-resolution, 15 kSamples.

The visual inspection confirms significant differences in the current comparison records. A change in frequency oscillation was observed, with the full-wave current showing a slightly lower oscillation frequency than the reduced-wave current. The change in the intensities is not so prominent for the frequency. For the voltage signals comparison, the automated TRIMP software indicates no significant differences in modules. For the current signals, the automated TRIMP software indicates significant differences in the FFT, TF, and WT modules, indicating a difference in the signal's frequency contents.

Figure 7 shows all the module's screen captures.

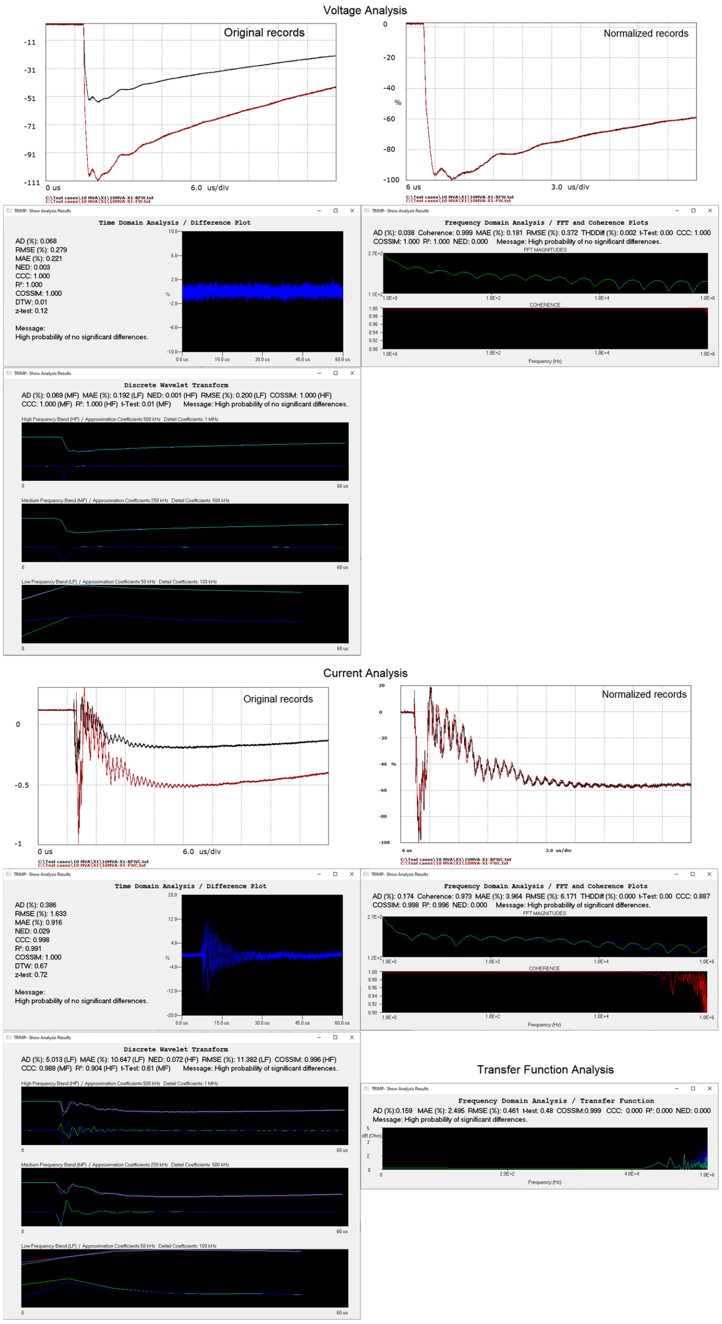

Figure 7. TRIMP software screen captures for Test Case 3. Different colored lines represent calculations for reduced and full impulses.

5.4. Test Case 4—Transformer 1000 kVA—Terminal H1

Test case 4 presents another chopped impulse test on a three-phase dry transformer, 1000 kVA, Dy, 13.8 kV/0.6 kV, BIL 110 kV—terminal under test H1. Signals are sampled at 75 MSamples/s with 9 bits-resolution, 32 kSamples.

In this test case, there are offset issues once the used oscilloscope is not adequately compensated to perform the tests.

Visual comparison of records and normalization clearly reveals the offset displacement. The TRIMP modules TIME and WT indicate significant differences when comparing such records. After choosing automatic offset adjustment, the TRIMP software shows no significant differences across all modules.

Figure 8 shows the module's screen captures illustrating the case.

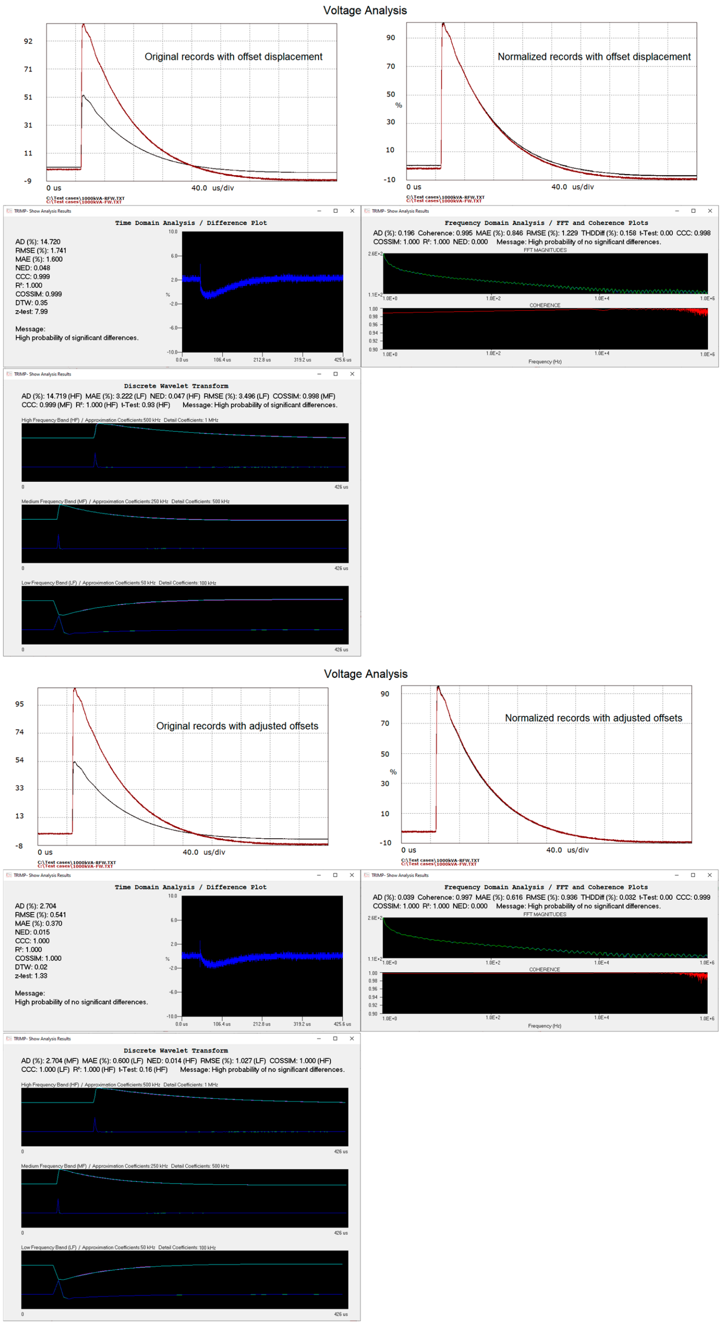

Figure 8. TRIMP software screen captures for Test Case 4. Different colored lines represent calculations for reduced and full impulses.

5.5. Test Case 5—Transformer 45 kVA—Chopped Test on Terminal H2

Test case 5 refers to a chopped impulse test on a three-phase transformer distribution transformer, 45 kVA, Dy, 13.8 kV/0.22 kV, BIL 110 kV, terminal under test H2. Voltage and current were sampled at 120 MSamples/s, 12 bits-resolution, 2.4 kSamples.

This test case demonstrates comparisons of chopped impulses, where the time to chop is identical between the signals.

Visual inspection confirms no significant differences among all voltage and current records. The TRIMP software also indicates no significant differences in all modules—TIME, FFT, TF, and WT—using the total record time of 40 µs.

Figure 9 shows the module's screen captures.

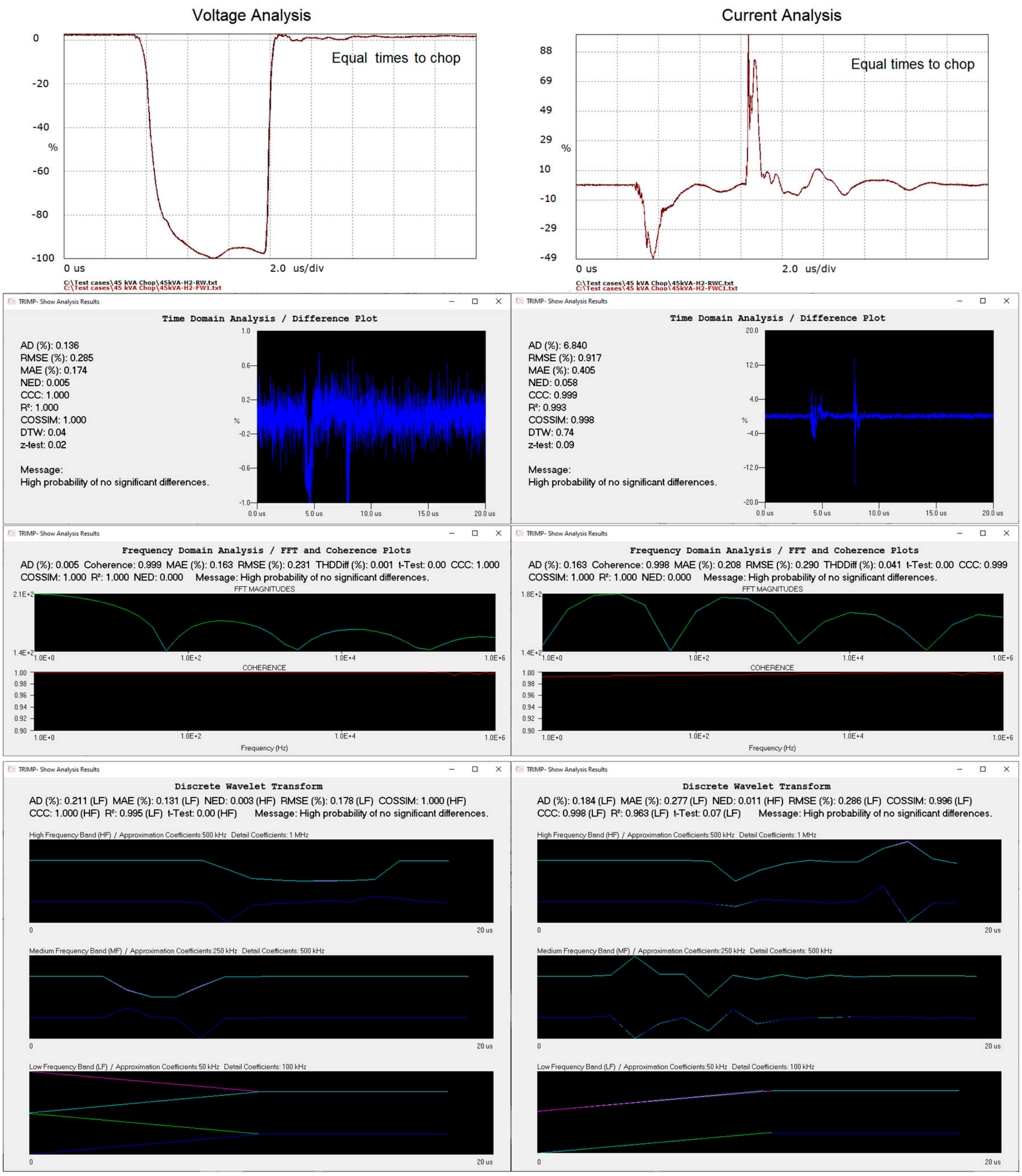

Figure 9. TRIMP software screen captures for Test Case 5. Different colored lines represent calculations for reduced and full impulses.

5.6. Test Case 6—Transformer 500 kVA—Chopped Test on Terminal H1—Full Comparison

Test case 6 presents another chopped impulse test on a three-phase dry transformer distribution transformer, 500 kVA, Dy, 13.8 kV/0.22 kV, BIL 110 kV—terminal under test H1. Voltage and current were sampled at 250 MSamples/s, 10 bits-resolution, 20 kSamples.

This test case demonstrates comparisons involving chopped impulses, where a significant difference in chopping time occurred. The chopping time from the virtual origin of the impulse is 3.6 µs for the reduced-voltage chopped impulse, compared to 2.1 µs for the full-voltage chopped impulse.

Visual inspection confirms no significant differences among all voltage and current records before chopping. However, differences were observed afterwards, as subsequent oscillations following the voltage collapse in the current records resulted in a different frequency oscillation. All modules in the TRIMP software indicate significant differences. Figure 10 shows the module's screen captures.

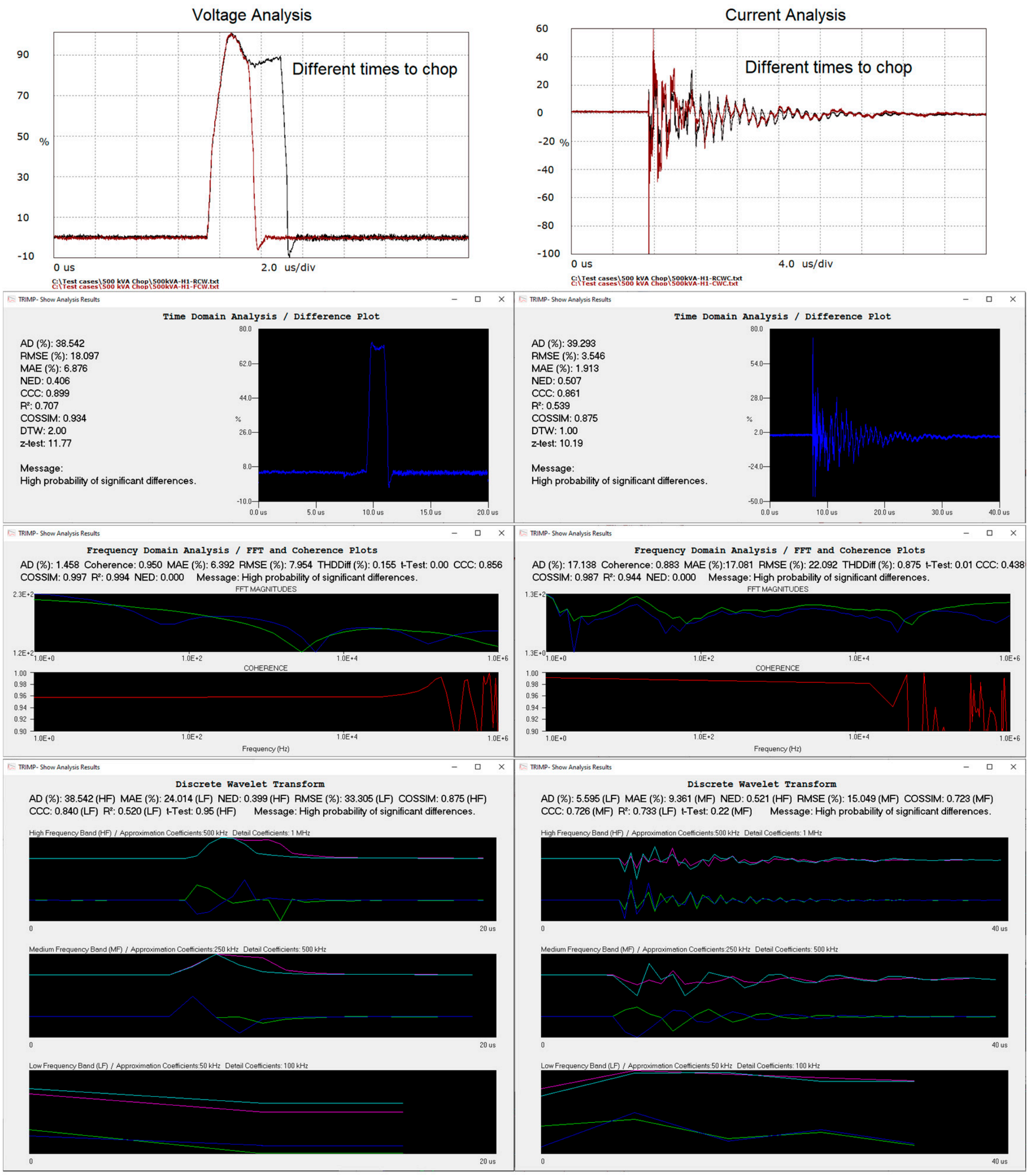

Figure 10. TRIMP software screen captures for Test Case 6. Different colored lines represent calculations for reduced and full impulses.

5.7. Test Case 7—Transformer 500 kVA—Chopped Test on Terminal H1—Limited Time Comparison

In the previous test case, comparisons were performed over the entire available signal recording period.

Typically, when comparisons involving chopped impulses with different times to chop are required, they are performed until the time of the fastest chop.

In Test Case 7, based on the actual time records starting from zero, the earliest time at which voltage collapse occurs for the full wave signal is 9.4 µs. Therefore, comparisons were made up to this shortest time to identify any significant differences prior to the chopping event. By comparing the records within this limited time frame, the TRIMP software shows no significant differences across all modules: TIME, FFT, and WT.

Figure 11 shows the module's screen captures for these circumstances.

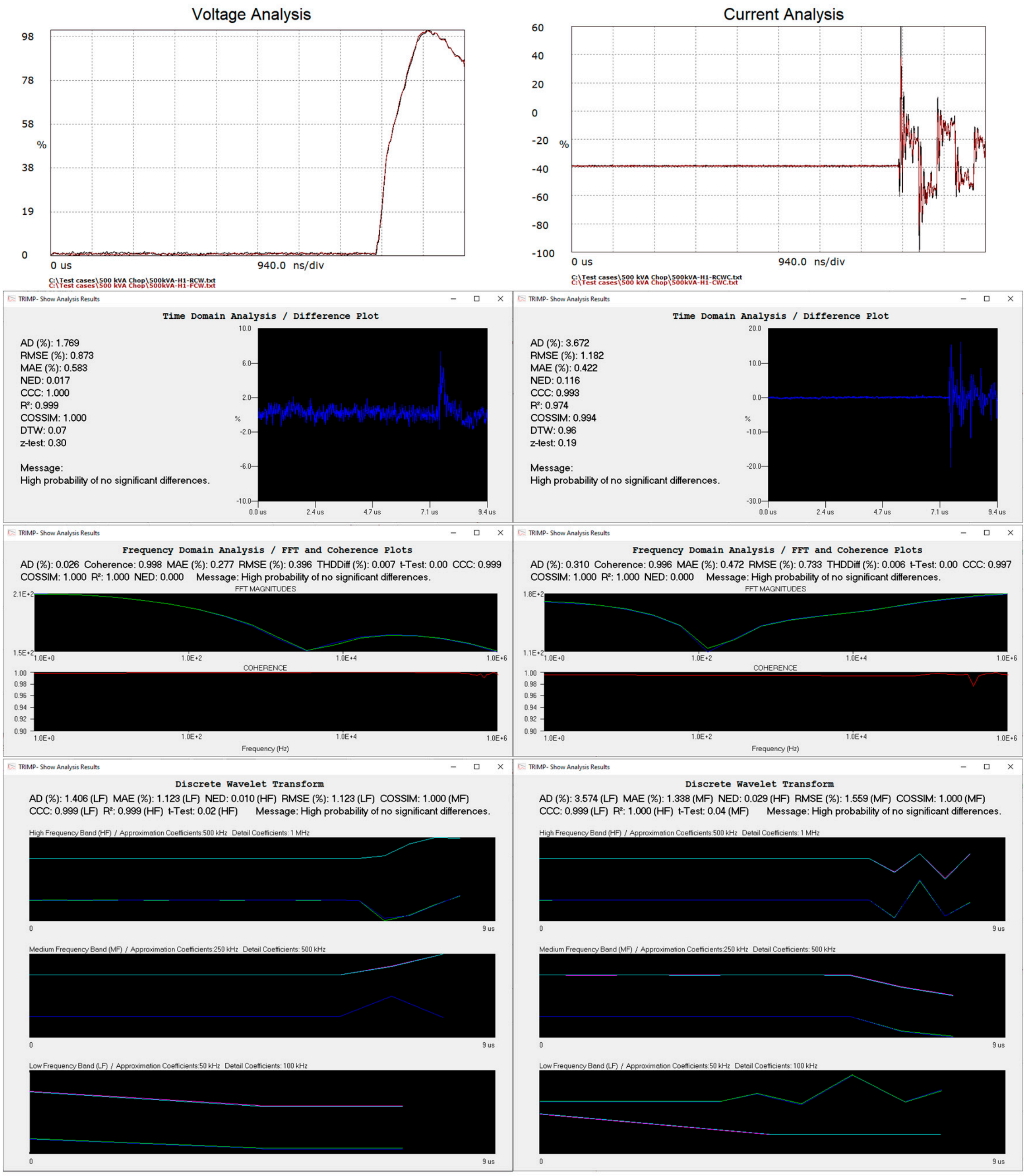

Figure 11. TRIMP software screen captures for Test Case 7. Different colored lines represent calculations for reduced and full impulses.

5.8. Test Case 8—Transformer 1000 kVA—Terminal X1

Test case 8 examines the current records for a three-phase transformer, 1000 kVA, Dy, 15 kV/0.22 kV, BIL 125 kV terminal under test H1. Records are sampled at 250 MSamples/s, 10 bits-resolution, 32 kSamples.

The currents, particularly the reduced one, exhibit significant noise, which may be due to an unfavorable attenuation ratio on the digitizer. Visually, the comparison of the raw signals indicates that the currents do not show significant differences; however, the presence of noise superimposed on the signals hinders clear visualization. The comparisons performed by the TIME and WT modules in the TRIMP software indicate significant differences. After applying the digital filter with a cutoff frequency of 5 MHz, both signals reveal strong concordance, and all modules in TRIMP confirm it.

Figure 12 displays screenshots from the modules, illustrating this situation.

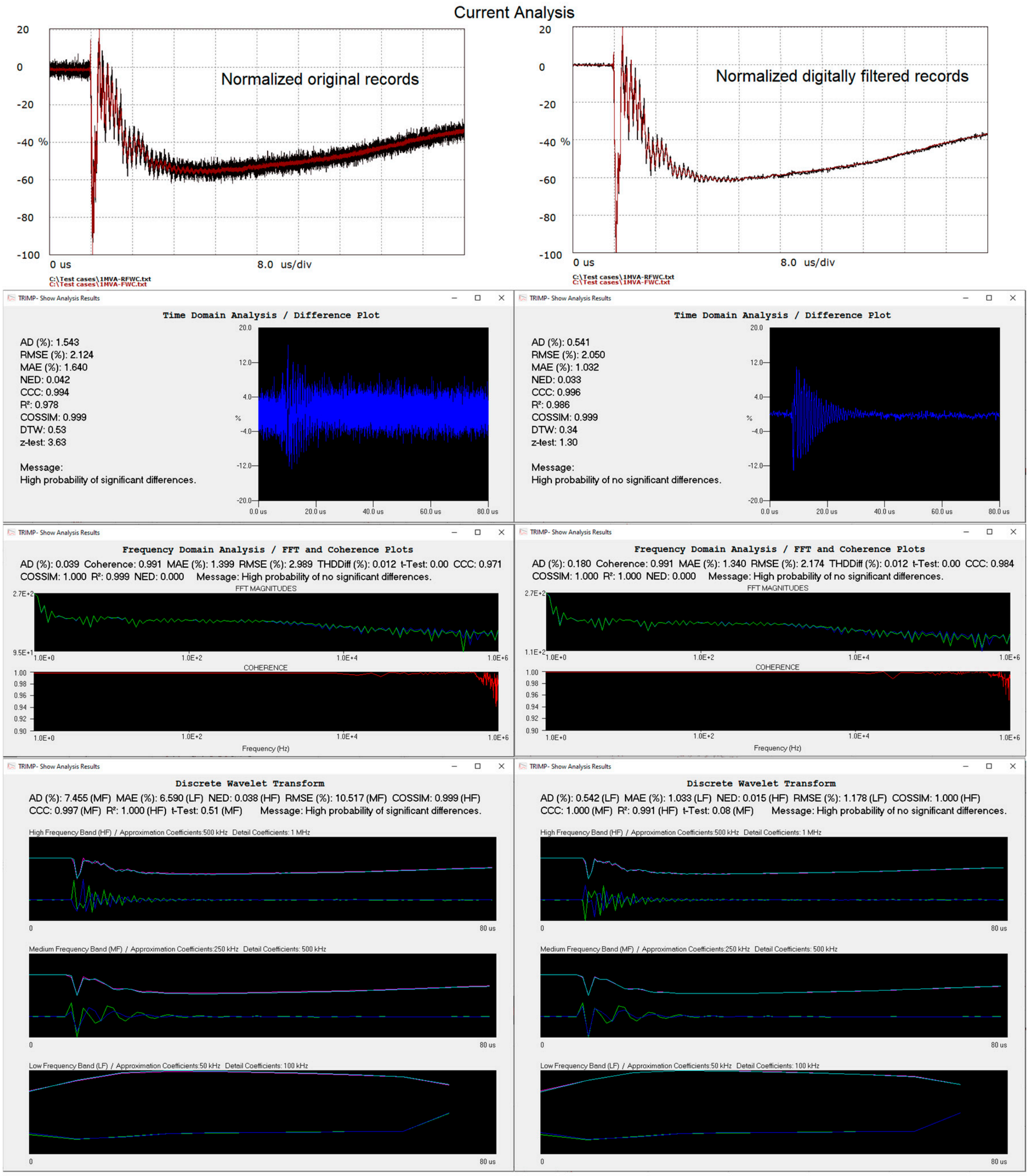

Figure 12. TRIMP software screen captures for Test Case 8. Different colored lines represent calculations for reduced and full impulses.

6. Discussion

The results obtained from the application of the TRIMP software confirm its effectiveness in detecting significant differences between test signals in both the time and frequency domains.

The results indicating the presence or absence of significant differences between signal records—both voltage and current—were consistent with visual observations. The combination of metrics used was satisfactory, and although there are redundancies in the selection of metrics, the computational cost is negligible because sequential calculations leverage partial computations from one metric to another.

The conservative interpretation is that if only some of the modules indicate significant differences, this should be considered the overall result of the test, leading to appropriate actions to investigate these differences, which are in line with established practices.

In Test Case 1 the module results did not indicate significant differences between the voltage and current signal recordings, corroborating the visual inspection that also did not identify discrepancies. This demonstrates that TRIMP maintains consistency in results when there are no real faults to be detected, validating its ability to operate in standard test scenarios.

The DTW (Dynamic Time Warping) choice for time-domain analysis proves to be important. Test Case 2 demonstrates a subtle, short-duration change that is not detectable by average, deviation, or correlation metrics.

Frequency-domain analyses are important because, as a rule, insulation failures lead to changes in oscillation frequencies. Test Case 3 illustrates a situation where no time-domain metric detected the frequency changes indicated by the FFT, FT, and WT modules.

Test Case 4 deals with offset shift in the signals, caused by inadequate oscilloscope compensation. Visual inspection showed discrepancies, but after applying automatic offset correction using the TRIMP software, the signals were adjusted, and no significant differences were detected by the analysis modules (TIME, FFT, and WT). This case highlights TRIMP's effectiveness in correcting measurement errors and preventing false fault indications, ensuring more accurate and objective test analysis.

Test Cases 5, 6, and 7, involving chopped waves, present specific features related to chop times. The analysis is also feasible and well-executed with the tools, and the results are adequate and consistent with visual observations. In Test Case 5, the software confirmed no significant differences between the voltage and current signals in the chopped impulse test when the times to chop were similar. In Test Case 6, the software indicated significant differences in the records, especially after the voltage collapse, showing a difference in the oscillation frequency of the recorded currents. In Test Case 7, a comparison limited to the moment of the fastest chop revealed that, prior to the chopping event, the signals showed no significant differences, validating TRIMP's flexible application for different comparison approaches.

Test Case 8, which exhibited significant noise in the current signals due to an unfavorable attenuation ratio in the measurement system, demonstrated the effectiveness of applying digital filters. Although the noise made it difficult to clearly visualize discrepancies, the use of digital filtering with an appropriate cutoff frequency allowed for the validation of comparisons that were previously masked by the noise. This case highlights how digital pre-processing is a critical step in impulse test analysis, especially in noisy environments.

In all tested cases, the WT (Wavelet Transform) module was the only one that matched the visual observations in indicating the presence or absence of significant differences. The ability to analyze both time and frequency information simultaneously al-lows for the detection of differences in signals that may vary over time and across different frequency bands. This suggests that such an algorithm should be promoted and even recommended in future editions of normative documents.

7. Conclusions

This article reviewed impulse test evaluation practices and presented the development of a comprehensive automated decision-making software tool for power transformer testing.

The initial review has shown that, even after several decades (in fact, almost a century) of industrial impulse testing of transformers and reactors, the tremendous evolution of digital capacities on acquisition, processing, and algorithms that are available nowadays, and the standardized procedures regarding pass/fail criteria still hold on visual comparisons involving some subjectivity, personal skills, adjustments and judgments, which often leads to disputes between manufacturers and purchasers, sending the experts to the testing laboratory.

The brief historical background presented also aimed to revisit the past and to illustrate to the professionals involved in this field and how the equipment used to record transients during tests has evolved. Despite advancements, a photographic-type approach is still used to evaluate results.

Disturbances such as offsets, trigger discrepancies, time shifts, and high-frequency oscillations pose significant challenges when performing impulse test comparisons of digital records. Addressing these disturbances requires a comprehensive understanding of their origins and effects, and meticulous attention to instrumentation setup, calibration, and data processing techniques. The automated correction employed demonstrates the importance of pre-processing tools in ensuring that test results reflect actual transformer conditions rather than measurement imperfections.

Thus, the TRIMP software was developed to emulate a photographic environment, allowing recorded waveforms to be placed and adjusted along the time and magnitude axes for visual comparison while adhering to standardized procedures to observe significant differences in superimposed images. Additionally, it implements robust numerical analysis to automate decision making. The software implements pre-processing smoothing and digital low-pass filtering, helping minimize noise and/or high disturbing frequencies.

All indicators of significant differences rely on comparison metrics with default thresholds. However, users can adjust the sensitivity of the comparisons by modifying the default values.

The record comparisons can be performed manually or visually, or through analysis in the time and frequency domains, using several algorithms and similarity and dissimilarity metrics on four modules.

Besides metrics and statistical calculations, the Dynamic Time Warp algorithm was implemented on the time domain module, revealing a valuable tool for analyzing and comparing the time-based data from the testing records.

On the frequency domain, the components of the Fast Fourier Transformer module calculations are extensively compared and tested, including using the Transfer Function module derived from the voltage/current recorded.

The Wavelet analysis module has proven to be a versatile and powerful tool for signal analysis, enabling more nuanced assessments of transformer test data. Unlike Fourier methods, which provide only frequency information, wavelets deliver localized time-frequency data, allowing for a detailed examination of signals across multiple scales. This ability to analyze both time and frequency information simultaneously permits the detection of differences in signals that may evolve over time or across different frequency bands, providing greater insight into transient phenomena. Given these capabilities, its use should be encouraged further. As wavelet analysis continues to evolve, its applications in signal processing will likely expand, becoming a recommended method in future editions of normative documents for power transformer testing.

The article discussed some of the many test cases processed during software development, showing all the inputs and outputs for different situations and presenting the module's responses. The modules and the associated metrics in each one can differently indicate the occurrence of significant differences between the signals.

The threshold values were selected as notable values that ensured the reproducibility of indications of significant differences, or lack thereof, throughout the research development and can be adjusted to infer greater or lesser sensitivity to decision indications.

The methodology and metrics employed can be utilized in machine learning systems, including techniques such as Artificial Neural Networks (ANNs) and other artificial intelligence (AI) approaches. Any AI or machine learning technique implementation begins with a foundation in well-established numerical methodologies, ensuring that predictive models are grounded in robust, validated analysis.

These systems can be trained to recognize patterns in impulse test data, thereby improving the detection of subtle differences between test records. Machine learning models are trained by processing large datasets, where algorithms learn from historical impulse data, adjusting internal parameters through iterative optimization to enhance prediction accuracy. This allows the model to reduce subjectivity in traditional methods and achieve more precise and automated transformer diagnostics. Several machine-learning approaches could enhance TRIMP's capabilities. Artificial Neural Networks (ANNs) could be trained on historical impulse test data to detect subtle differences between test records, supporting fault detection by identifying patterns in both normal and faulty responses and thus reducing subjectivity. Dynamic Time Warping (DTW), already in TRIMP, could be optimized with machine learning to recognize temporal variations linked to faults, refining its accuracy. Additionally, Wavelet Transform analysis could benefit from machine learning by identifying frequency bands or intervals indicative of faults, enabling predictive diagnostics. Finally, supervised models like Support Vector Machines (SVM) or Random Forests could classify results based on fault data, making TRIMP a semi-automated expert system for predicting fault likelihoods based on past test trends.

Future developments can enhance the software's capabilities, enabling more accurate and automated test evaluations. Intercomparisons among test laboratories and further standard development efforts are essential to achieve and establish improvements.

Nevertheless, besides full decision-making automation, the developed TRIMP software leads to the production of high-quality records and analysis images. The test assessment can state whether any differences between the records are significant based on the current standard practices and the expertise and knowledge existing in testing laboratories.

8. Patent

Registered software

Bassi W, inventor; Bassi W, assignee. TRIMP—Record Comparison Software for Impulse Testing in High Voltage Transformers and Reactors (in Portuguese). Brazilian patent BR512024001730-5. 28 May 2024. Patent Office: INPI—Instituto Nacional da Propriedade Industrial.

Funding: This research received no external funding.

Data Availability Statement: The raw data supporting the conclusions of this article will be made available by the author on request.

Conflicts of Interest: The author declares no conflict of interest.

References

1. Vogel, F.J.; Montsinger, V.M. Impulse testing of commercial transformers. *Electr. Eng.* **1933**, *52*, 9–11. [CrossRef]
2. Vogel, F.J.; Montsinger, V.M. Progress Report on Impulse Testing of Commercial Transformers. *Trans. Am. Inst. Electr. Eng.* **1933**, *52*, 409–410. [CrossRef]
3. Hagenguth, J.H. Progress in Impulse Testing of Transformers. *Trans. Am. Inst. Electr. Eng.* **1944**, *63*, 999–1005. [CrossRef]
4. *AIEE No 13-1930*; AIEE Transformers, Induction Regulators and Reactors. IEEE: New York, NY, USA, 1930; pp. 1–22. [CrossRef]
5. Aicher, L.C. Experience with Transformer Impulse Failure Detection Methods. *Trans. Am. Inst. Electr. Eng.* **1948**, *67*, 1621–1631. [CrossRef]
6. Ramachandran, P. Standards relevant to transformers—Part II. In *Transformers Magazine*; Merit Media Int: Zagreb, Croatia, 2020; Volume 7. Available online: https://hrcak.srce.hr/en/file/352105 (accessed on 25 August 2024).
7. Treanor, E.D.; Stewart, H.C.; Holcomb, J.E. Production impulse testing of distribution transformers. *Electr. Eng.* **1952**, *71*, 925–928. [CrossRef]
8. *IEC 76-1*; Power Transformers Part 1: General. International Electrotechnical Commission: London, UK, 1976.
9. Stewart, H.C.; Holcomb, J.E. Impulse-Failure-Detection Methods as Applied to Distribution Transformers. *Trans. Am. Inst. Electr. Eng.* **1945**, *64*, 640–644. [CrossRef]
10. Rippon, E.C.; Hickling, G.H. The detection by oscillographic methods of winding failures during impulse tests on transformers. *J. Inst. Electr. Eng.—Part II Power Eng.* **1949**, *96*, 769–778. [CrossRef]
11. *IEC 60076-3*; Power Transformers—Part 3: Insulation Levels, Dielectric Tests and External Clearances in Air. International Electrotechnical Commission: London, UK, 2013.
12. *IEC 60076-4*; Power Transformers—Part 4: Guide to the Lightning Impulse and Switching Impulse Testing—Power Transformers and Reactors. International Electrotechnical Commission: London, UK, 2002.
13. Malewski, R.; Poulin, B. Impulse testing of power transformers using the transfer function method. *IEEE Trans. Power Deliv.* **1988**, *3*, 476–489. [CrossRef]
14. Malewski, R.; Gokenbach, E.; Maeier, R.; Fellmann, K.H.; Claudi, A. *Five Years of Monitoring the Impulse Test of Power Transformers with Digital Recorders and the Transfer Function Method*; Paper 12-201; CIGRE: Paris, France, 1992; pp. 1–6.
15. *IEEE Std C57.98*; IEEE Guide for Transformer Impulse Tests. The Institute of Electrical and Electronics Engineers IEEE: New York, NY, USA, 2011. [CrossRef]
16. Leibfried, T.; Feser, K. Monitoring of power transformers using the transfer function method. *IEEE Trans. Power Deliv.* **1999**, *14*, 1333–1341. [CrossRef]
17. Arunkumar, S.; Sandeep, V.; Shankar, S.; Gopalakrishnan, M.; Udayakumar, K.; Jayashankar, V. Impulse testing of power transformers—A model reference approach. *IEE Proc.—Sci. Meas. Technol.* **2004**, *151*, 25–30. [CrossRef]
18. Purkait, P.; Chakravorti, S. Time and frequency domain analyses based expert system for impulse fault diagnosis in transformers. *IEEE Trans. Dielectr. Electr. Insul.* **2002**, *9*, 433–445. [CrossRef]
19. Handreck, K.; Dabke, K.P.; Conlon, M.F. An expert system for transformer impulse test diagnosis. *Eng. Appl. Artif. Intell.* **1991**, *4*, 11–21. [CrossRef]
20. Wood, A.B. The Cathode Ray Oscillograph. *Proc. Phys. Soc. Lond.* **1922**, *35*, 109. [CrossRef]
21. Wolff, O.; Hawkes, P. Chapter Fourteen—From the cathode-ray oscillograph to the high-resolution electron microscope. In *Advances in Imaging and Electron Physics*; Peter, W., Hawkes, M.H., Eds.; Elsevier: Amsterdam, The Netherlands, 2022; Volume 221, pp. 443–468. [CrossRef]
22. Dufour, A. Oscillographe cathodique. *J. Phys. Radium.* **1920**, *1*, 147–160. [CrossRef]
23. Thomas, J.B. *Transformers at Pittsfield: A History of the General Electric Large Power Transformer Plant at Pittsfield*; Gateway Press: Wareham, MA, USA, 1998; 336p.
24. ETHW Engineering and Technology History Wiki—IEEE History Center. Archives: Transformers at Pittsfield, Part 2. Available online: https://ethw.org/Archives:Transformers_at_Pittsfield,_part_2 (accessed on 27 August 2024).
25. Norinder, H. The Cathode Oscillograph as Used in the Study of Lightning and Other Surges on Transmission Lines. *Trans. Am. Inst. Electr. Eng.* **1928**, *47*, 446–455. [CrossRef]
26. Ackermann, O. A Cathode Ray Oscillograph with Norinder Relay Its Design and Application. *Trans. Am. Inst. Electr. Eng.* **1930**, *49*, 467–474. [CrossRef]
27. Lecroy, W. Progress in Electronic Technologies: From early particle physics to modern signal processing. In Proceedings of the XIV LNF Spring Scholl "Bruno Touschek" in Nuclear, Subnuclear and Astroparticle Physics Conference, Frascati, Italy, 11–15 May 2009. Available online: https://www.lnf.infn.it/conference/lnfss/09/slides/LeCroy.pdf (accessed on 27 August 2024).
28. *IEEE 1122-1987*; Standard for Digital Recorders for Measurements in High-Voltage Impulse Tests. The Institute of Electrical and Electronics Engineers IEEE: New York, NY, USA, 1987. [CrossRef]
29. *IEC 61083-1*; Digital Recorders for Measurements in High-Voltage Impulse Tests Part 1: Requirements for Digital Recorders. International Electrotechnical Commission: London, UK, 1993.

30. *IEC 61083-2*; Digital Recorders for Measurements in High-Voltage Impulse Tests Part 2: Evaluation of Software Used for the Determination of the Parameters of Impulse Waveforms. International Electrotechnical Commission: London, UK, 1997.
31. McComb, T.R.; Schon, K.; Malewski, R.A. Standards for digital recorders for measurements in high-voltage impulse tests. *Comput. Stand. Interfaces* **2000**, *22*, 89–99. [CrossRef]
32. Dikun, J.; Onal, E. Coherence and time-frequency analysis of impulse voltage and current measurements. *J. Energy S. Afr.* **2015**, *26*, 118–122. Available online: http://www.scielo.org.za/scielo.php?script=sci_arttext&pid=S1021-447X2015000200013 (accessed on 26 August 2024). [CrossRef]
33. Jeng, Y.C. Digital spectra of non-uniformly sampled signals: Theories and applications. I. Fundamentals and high speed waveform digitizers. 1988. IMTC-88. In Proceedings of the 5th IEEE Instrumentation and Measurement Technology Conference, San Diego, CA, USA, 20–22 April 1988; pp. 391–398. [CrossRef]
34. Jenq, Y.C. Digital spectra of nonuniformly sampled signals. II. Digital look-up tunable sinusoidal oscillators. *IEEE Trans. Instrum. Meas.* **1988**, *37*, 358–362. [CrossRef]
35. Johnson, J.B. Thermal agitation of electricity in conductors. *Phys. Rev.* **1928**, *32*, 97–109. [CrossRef]
36. Der Ziel, A.V. Thermal Noise in Field-Effect Transistors. *Proc. IRE* **1962**, *50*, 1808–1812. [CrossRef]
37. Kapusta, R.; Zhu, H.; Lyden, C. Sampling Circuits That Break the KT/c Thermal Noise Limit. *IEEE J. Solid-State Circuits* **2014**, *49*, 1694–1701. [CrossRef]
38. *IEC 60060-1*; High-Voltage Test Techniques—Part 1: General Definitions and Test Requirements. International Electrotechnical Commission: London, UK, 2010.
39. *IEEE 1112*; IEEE Standard for Digital Recorders for Measurements in High-Voltage Impulse Tests. The Institute of Electrical and Electronics Engineers IEEE: New York, NY, USA, 1998. [CrossRef]
40. Bassi, W. TRIMP—Record Comparison Software for Impulse Testing in High Voltage Transformers and Reactors. Brazilian Patent BR512024001730-5, 28 May 2024. Patent Office: INPI—Instituto Nacional da Propriedade Industrial. (In Portuguese)
41. Skiena, S.S. *The Algorithm Design Manual*; Springer Nature, B.V.: Berlin/Heidelberg, Germany, 2021; ISBN 9783030542580.
42. Yelamanchi, D.; Aravind, K.A.; Marimuthu, K.; Pandian, G. Analysis of Transformer Impulse Test Signals using Transfer and Coherence Functions. In Proceedings of the 2024 Fourth International Conference on Advances in Electrical, Computing, Communication and Sustainable Technologies (ICAECT), Bhilai, India, 11–12 January 2024; pp. 1–5. [CrossRef]
43. Satish, L. Short-time Fourier and wavelet transforms for fault detection in power transformers during impulse tests. *IEE Proc.—Sci. Meas. Technol.* **1998**, *145*, 77–84. [CrossRef]
44. Tan, P.N.; Steinbach, M.; Karpatne, A.; Kumar, V. *Introduction to Data Mining*, 2nd ed.; Pearson Education: New York, NY, USA, 2019; ISBN 9780133128901.
45. Angrisani, L.; Daponte, P.; Dias, C.; Vale, A. Advanced Processing Techniques of High-Voltage Impulse Test Signals. *IEEE Trans. Instrum. Meas.* **1998**, *47*, 439–445. [CrossRef]
46. Yang, Q.; Su, P.; Chen, Y. Comparison of Impulse Wave and Sweep Frequency Response Analysis Methods for Diagnosis of Transformer Winding Faults. *Energies* **2017**, *10*, 431. [CrossRef]
47. Deza, M.M.; Deza, E. *Encyclopedia of Distances*; Springer: Berlin/Heidelberg, Germany, 2012; ISBN 978-3-642-30957-1.
48. Brown, M.; Rabiner, L. Dynamic time warping for isolated word recognition based on ordered graph searching techniques. ICASSP '82. In Proceedings of the IEEE International Conference on Acoustics, Speech, and Signal Processing, Paris, France, 3–5 May 1982; pp. 1255–1258. [CrossRef]
49. Phan, T.T.H.; Poisson Caillault, É.; Lefebvre, A.; Bigand, A. Dynamic time warping-based imputation for univariate time series data. *Pattern Recognit. Lett.* **2020**, *139*, 139–147. [CrossRef]
50. Vasimalla, K.; Challa, N.; Manohar Naik, S. Efficient dynamic time warping for time series classification. *Indian J. Sci. Technol.* **2020**, *9*, 1–7. [CrossRef]
51. Sakoe, H.; Chiba, S. Dynamic programming algorithm optimization for spoken word recognition. *IEEE Trans. Acoust. Speech Signal Process.* **1978**, *26*, 43–49. [CrossRef]
52. Cooley, J.; Tukey, J. An Algorithm for the Machine Calculation of Complex Fourier Series. *Math. Comput.* **1965**, *19*, 297–301. [CrossRef]
53. Reddy, K.S.; Kumar, M.P.V.V.R.; Singh, B.P.; Suryakalavathi, M. Coherence function method of detection of fault in a power transformer during impulse test. In Proceedings of the 2011 International Conference on Power and Energy Systems, Chennai, India, 22–24 December 2011; pp. 1–6. [CrossRef]
54. Müller, S. Measuring Transfer-Functions and Impulse Responses. In *Handbook of Signal Processing in Acoustics*; Havelock, D., Kuwano, S., Vorländer, M., Eds.; Springer: New York, NY, USA, 2008. [CrossRef]
55. Rioul, O.; Vetterli, M. Wavelets and signal processing. *IEEE Signal Process. Mag.* **1991**, *8*, 14–38. [CrossRef]
56. Daubechies, I. *Ten Lectures on Wavelets*; Society for Industrial and Applied Mathematics: Philadelphia, PE, USA, 1992; ISBN 978-089871274.

57. Morlet, J.; Arens, G.; Fourgeau, E.; Giard, D. Wave propagation and sampling theory—Part I: Complex signal and scattering in multilayered media. *Geophysics* **1982**, *47*, 203–221. [CrossRef]
58. Mallat, S.G. A theory for multiresolution signal decomposition: The wavelet representation. *IEEE Trans. Pattern Anal. Mach. Intell.* **1989**, *11*, 674–693. [CrossRef]
59. Bulnes, F. *Recent Advances in Wavelet Tansforms and Their Applications*; IntechOpen: London, UK, 2022; ISBN 978-1-80355-739-7.
60. Haar, A. Zur Theorie der orthogonalen Funktionensysteme. *Math. Ann.* **1910**, *69*, 331–371. [CrossRef]
61. Smith, S.W. *The Scientist and Engineer's Guide to Digital Signal Processing*, 2nd ed.; California Technical Publishing: San Diego, CA, USA, 1999; ISBN 0-9660176-7-6.
62. Litovski, V. Chebyshev and Modified Chebyshev Filters. In *Electronic Filters. Lecture Notes in Electrical Engineering*; Springer: Singapore, 2019; Volume 596. [CrossRef]
63. Amgad, A.; AbdelAty, A.M.; Elbarawy, M.T.M.M.; Attia, H.A.; Radwan, A.G. Design of a Low-pass Filter from Fractional Chebyshev Polynomials. In Proceedings of the 2021 International Conference on Microelectronics (ICM), New Cairo City, Egypt, 19–22 December 2021; pp. 144–147. [CrossRef]